TABLE 1. Selective Inhibitory Effect of Y-39983 on ROCK

Compounds	IC_{50} (μM)		
	ROCK	PKC	CaMKII
Y-39983	0.0036 (0.0025–0.0051)	0.42 (0.36–0.49) [117 times]	0.81 (0.67–0.97)] [225 times]
Y-27632	0.11 (0.074–0.17)	9.0 (7.1–11) [82 times]	26 (21–32) [236 times]
Staurosporine	0.0011 (0.00078–0.0015)	0.00026 (0.00024–0.00030) [0.24 times]	0.00036 (0.00033–0.00040) [0.33 times]

In parentheses, 95% confidence interval; in brackets, comparison with the IC_{50} of ROCK.

weeks ($n = 8$). In slit lamp examinations, the cornea (epithelial defects revealed by fluorescein biostaining, opacity, and neovascularization), conjunctiva (hyperemia, swelling), anterior chamber (flare), and iris (hyperemia, swelling) were observed. The lens, vitreous, and retina were observed in eyes under mydriasis, with a slit lamp and binocular indirect ophthalmoscope. Tear quantity was measured by phenol red thread (Zonequick; Menicon, Nagoya, Japan). The electroretinogram (ERG) was measured to evaluate retinal safety. In darkness and under mydriasis with systemic anesthetization, a contact lens-type electrode was fitted to the eye. Results of light stimulation and the ERG were recorded using a veterinary ERG system. Amplitudes of the a- and b-waves and the peak latency were determined. In addition, histologic examination was performed by the usual method after the last observation. The tissues observed were the eye including the palpebral and bulbar conjunctiva, and optic nerve, lacrimal glands, internal organs including the liver, gallbladder, kidneys, spleen, heart, aorta, gullet, stomach, intestines, lungs, and bronchial tube, sex organs, brain, bone, muscle, skin, and other tissues.

In addition, to investigate the safety of Y-39983 at various frequencies of administration, the drug was administered two and three times a day (BID and TID) to rabbits and monkeys. In rabbits in the BID study, 0.05% or 0.1% Y-39983 or saline was topically administered to both eyes twice daily (with a 6-hour interval) for 4 weeks ($n = 3$). In rabbits in the TID study, 0.1% Y-39983 or saline was topically administered three times a day at 5-hour intervals for 2 weeks ($n = 5$). In monkeys in the BID study, 0.05%, 0.1%, or 0.2% Y-39983 or saline was topically administered twice daily at a 6-hour interval for 4 weeks ($n = 3$). Ocular tissues were observed in the same fashion as for administration four times a day.

Effects on Cultured Human Umbilical Venous Endothelial Cells

Human umbilical venous endothelial cells (HUVECs) were purchased from Dainippon Pharmaceutical (Osaka, Japan). HUVECs were cultured in CS-C medium (Dainippon Pharmaceutical) and maintained in a 95% air-5% CO_2 atmosphere at 37°C and passaged using the trypsin-EDTA method. HUVECs were seeded into 24-well plates. After seeding, HUVECs were incubated in medium containing 1 μM Y-39983 for 15 or 30 minutes and observed by phase-contrast microscopy. Medium was then removed, and HUVECs were incubated in medium without Y-39983 for 1 hour to evaluate recovery from the morphologic changes induced by Y-39983.

RESULTS

Selective Inhibitory Effect of Y-39983 on ROCK Activity

Results are summarized in Table 1. The 50% inhibitory concentration (IC_{50}) of Y-27632 for ROCK (0.11 μM; 95% CI, 0.074–0.17 μM), was 30.6 times that of Y-39983 (0.0036 μM; 95% CI, 0.0025–0.0051 μM). In contrast, in the examination of inhibition of PKC and CaMKII, the IC_{50}s of Y-27632 and Y-39983 for PKC were 9.0 μM (95% CI, 7.1–11 μM) and 0.42 μM (95% CI, 0.36–0.49 μM), respectively, whereas the IC_{50}s of Y-27632 and Y-39983 for CaMKII were 26 μM (95% CI, 21–32 μM) and 0.81 μM (95% CI, 0.67–0.97 μM), respectively. The IC_{50}s of Y-27632 and Y-39983 for PKC were 82 and 117 times those for ROCK, respectively, whereas the IC_{50}s of Y-27632 and Y-39983 for CaMKII were 236 and 225 times those for ROCK, respectively. In addition, the same experiments were performed as controls using staurosporine, a nonspecific protein kinase inhibitor. Staurosporine exhibited the same inhibitory effects on all three kinases—ROCK, PKC, and CaMKII—as shown in Table 1. These findings indicate that Y-39983 more potently inhibits ROCK than Y-27632 and has the same selectivity for ROCK as Y-27632. In addition, Y-39983 was more selective for ROCK than staurosporine.

IOP Measurements in Rabbit Eyes

In rabbits, Y-39983 lowered IOP in a dose-dependent fashion, as shown in Figure 2A. Statistically significant IOP-lowering effects were found at concentrations of Y-39983 equal to or higher than 0.01% at 2 hours after topical administration. IOP reduction was at maximum between 2 and 3 hours after administration of 0.01% to 0.1% Y-39983. Maximum IOP reduction (mean ± SE) was 2.5 ± 0.8 ($P = 0.28$ vs. vehicle-treated eyes, Williams' test, one-sided), 7.0 ± 1.6 ($P = 0.0009$), 11.0 ± 1.0 ($P < 0.0001$), 12.1 ± 1.5 ($P < 0.0001$), and 13.2 ± 0.6 ($P < 0.0001$) at 0.003%, 0.01%, 0.03%, 0.05%, and 0.1% Y-39983, respectively (Fig. 2B). This result demonstrated the potent IOP-lowering effects of Y-39983 in rabbit eyes.

In addition, repeated topical administration of 0.03% Y-39983 (four times a day) was performed in rabbit eyes. Figure 3 shows the time course of changes in peak IOP reduction over 28 days. Mean reduction of IOP was between 7.0 and 9.6 mm Hg during the 28-day period, demonstrating that maintenance of IOP reduction is obtained with repeated administration.

IOP Measurements in Monkey Eyes

In monkeys, Y-39983 dose dependently lowered IOP, as shown in Figure 4A. Compared with vehicle-treated eyes, 0.05% Y-39983-treated eyes in particular exhibited significant reduction of IOP between 2 and 7 hours after topical administration ($P < 0.05$, the Dunnett's test, one-sided). The reduction of IOP was at maximum 3 hours after administration of 0.05% Y-39983. The reductions of IOP (mean ± SE) at 2, 3, 5, and 7 hours after administration of 0.05% Y-39983 were 1.9 ± 0.3, 2.5 ± 0.4, 1.7 ± 0.3, and 0.8 ± 0.2 mm Hg, respectively. Maximum IOP reduction (mean ± SE) was 0.4 ± 0.1, 0.4 ± 0.2, 1.4 ± 0.3 ($P < 0.05$ vs. vehicle-treated eyes, Williams' test, one-sided),

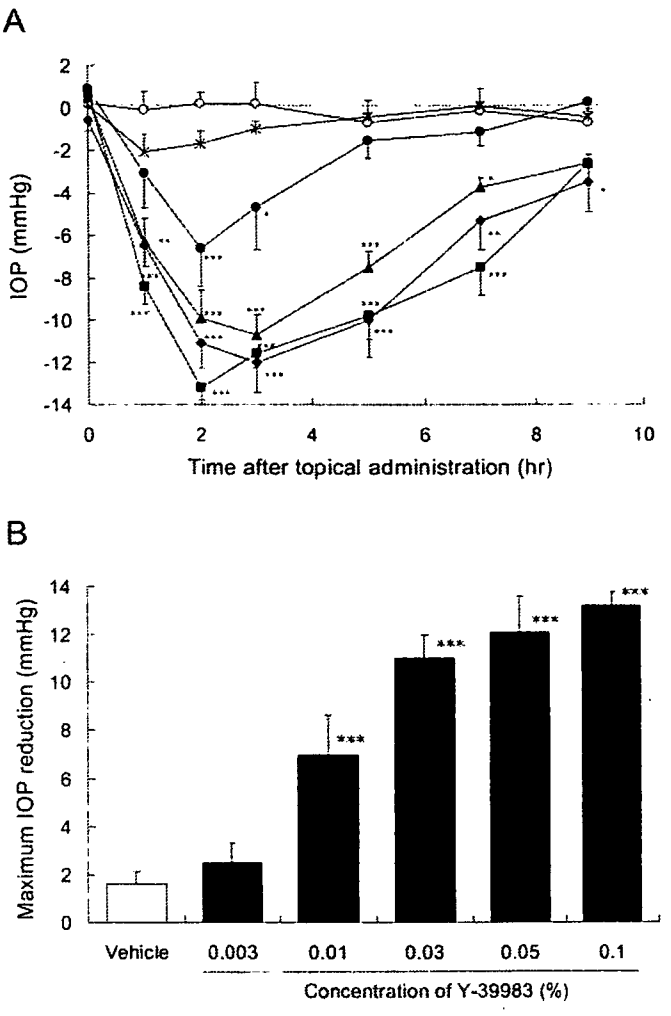

FIGURE 2. Effect of topical administration of Y-39983 on IOP in rabbit eyes. Y-39983 or its vehicle was topically administered to one eye in rabbits. The contralateral eyes were treated with the same volume of saline (n = 5). (A) Time course of changes in IOP. (○) Vehicle; (×) 0.003%; (●) 0.01%; (▲) 0.03%; (◆) 0.05%; and (■) 0.1% Y-39983. IOPs were calculated as the difference between the value in the Y-39983- or the vehicle-treated eye and the contralateral saline-treated eyes at each time point. Data are the mean mm Hg ± SE. The significance of findings was evaluated by the Dunnett's test (one-sided); $^{*}P < 0.05$, $^{**}P < 0.01$, and $^{***}P < 0.001$, compared with the vehicle group at each time point. (B) Maximum IOP reduction. Data are the mean mm Hg ± SE. The significance of findings was evaluated by the Williams' test (one-sided); $^{***}P < 0.001$, compared with the vehicle group. Baseline IOPs were 20.7 ± 0.9, 20.5 ± 1.2, 22.9 ± 0.6, 19.6 ± 0.5, 22.0 ± 0.6, and 21.5 ± 0.7 mm Hg (mean ± SE) with vehicle, 0.003%, 0.01%, 0.03%, 0.05%, and 0.1% Y-39983, respectively.

and 2.5 ± 0.8 mm Hg ($P < 0.05$) at 0.003%, 0.01%, 0.03%, and 0.05% Y-39983, respectively (Fig. 4B). Statistically significant reduction of IOP was obtained at concentrations of Y-39983 equal to or greater than 0.03%. Administration of 0.005% latanoprost lowered IOP by 2.5 ± 0.2 mm Hg ($P < 0.001$ vs. vehicle-treated eyes, t-test, one-sided), demonstrating that the IOP-lowering effect of 0.05% Y-39983 was similar to that of 0.005% latanoprost.

Measurements of Total Outflow Facility and Uveoscleral Outflow

Outflow facility was measured 2 hours after topical administration of 0.05% Y-39983, when maximum IOP reduction was observed. As summarized in Table 2, outflow facility (mean ± SE) in eyes treated with Y-39983 (0.168 ± 0.018 μL/min/mm Hg) was approximately 1.7 times (+65.5%) that in the contralateral, vehicle-treated eyes (0.111 ± 0.014 μL/min per mm Hg. This difference was significant ($P < 0.001$, paired t-test, one-sided). In contrast, there were no significant differences in uveoscleral outflow between eyes treated with Y-39983 and those treated with vehicle.

Ocular Toxicologic Effects of Topical Administration of Y-39983

Ocular toxicologic properties were evaluated for long-term topical administration of Y-39983. In the QID study, rabbit eyes were treated with 0.003% to 0.03% Y-39983 four times a day (at 2-hour intervals) for 4 weeks, and monkey eyes with 0.003% to 0.05% Y-39983 at the same dosage for 26 weeks. In neither species were significant abnormalities of the corneal surface, anterior chamber, lens, vitreous, or retina observed on slit lamp examination, nor were significant findings of toxicity detected on histologic examination. ERG analysis revealed no abnormalities in eyes treated with Y-39983 of either species. At week 4, thread-wetting values (mean millimeters ± SE) for rabbits determined by the phenol red thread method were 29.4 ± 1.7, 29.4 ± 0.9, 28.8 ± 1.0, and 29.0 ± 1.1 mm with saline, 0.003%, 0.01%, and 0.03% Y-39983, respectively. At week 25, the thread-wetting values in monkeys were 30.0 ± 1.0, 28.5 ± 1.0, 31.0 ± 0.7, 28.9 ± 1.1, and 29.1 ± 0.8 mm with vehicle, 0.003%, 0.01%, 0.03%, and 0.05% Y-39983, respectively. There were no differences in thread-wetting values between the groups of rabbits and monkeys. However, conjunctival hyperemia and punctate subconjunctival hemorrhage were observed in eyes with topical administration of Y-39983 in rabbits (Fig. 5A) and monkeys (Fig. 5B), and punctate subconjunctival hemorrhage was sporadic during the administration period in both species. In the QID study, punctate subconjunctival hemorrhages were observed in four of five rabbits receiving 0.03% Y-39983 and in two of eight monkeys receiving 0.05% Y-39983. The hemorrhages resolved during the administration period. However, in the BID and TID studies,

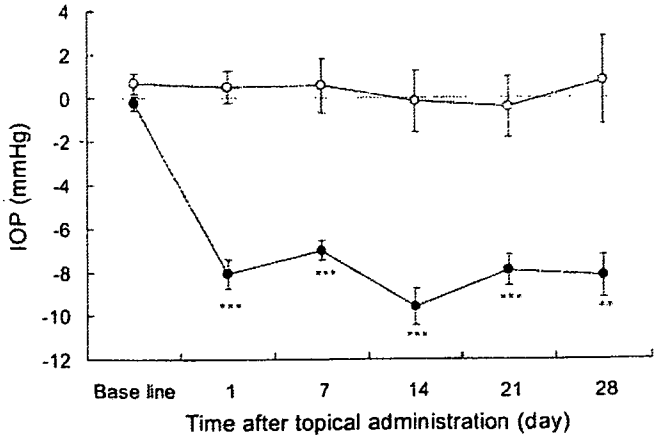

FIGURE 3. Effects of repeated topical administration of Y-39983 on IOP in rabbit eyes. Y-39983 0.03% or its vehicle was topically administered to one eye in rabbits four times a day for 28 days (n = 6). The contralateral eyes were not treated. IOPs were measured 2 hours after administration in the morning. (○) vehicle; (●) 0.03% Y-39983. IOPs were calculated as the difference between the value in the Y-39983 or vehicle-treated eye and the contralateral nontreated eye at each time point. Data are the mean mm Hg ± SE. The significance of findings was evaluated by t-test (one-sided); $^{**}P < 0.01$ and $^{***}P < 0.001$, compared with the vehicle group at each time point. Baseline IOPs were 20.9 ± 0.5 and 21.0 ± 0.5 mm Hg (mean ± SE) with vehicle and 0.03% Y-39983, respectively.

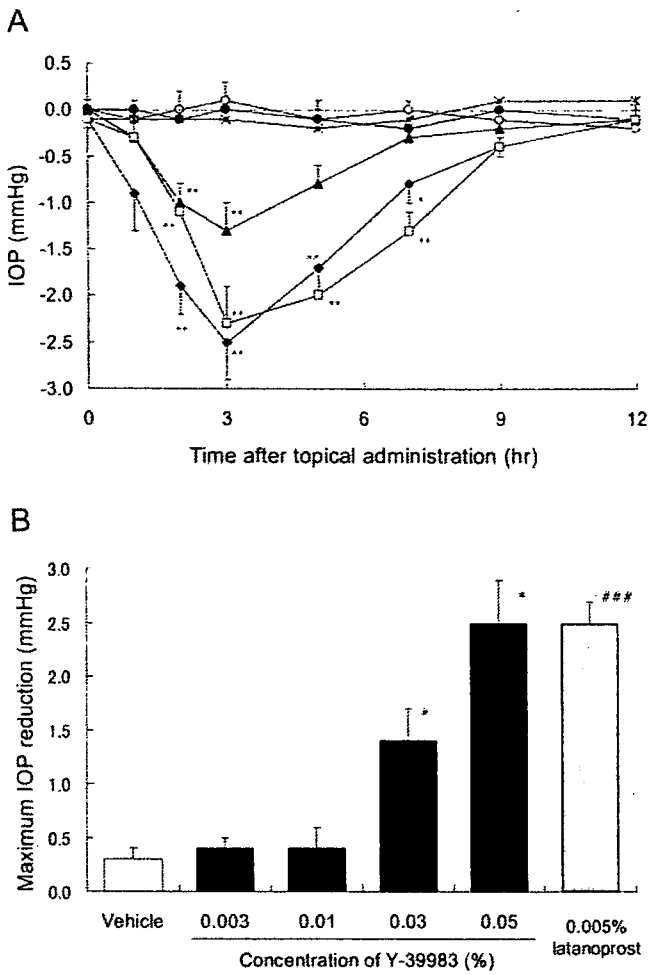

FIGURE 4. Effects of topical administration of Y-39983 on IOP in monkey eyes. Y-39983 or its vehicle was topically administered to one eye in monkeys. The contralateral eyes were treated with the same volume of saline (n = 5). (A) Time course of changes in IOP. (○) vehicle; (×) 0.003%; (●) 0.01%; (▲) 0.03%; and (◆) 0.05% of Y-39983; (□) 0.005% latanoprost. IOPs were calculated as the difference between the value in Y-39983 or vehicle-treated eyes and contralateral saline-treated eyes at each time point. Data are the mean mm Hg ± SE. The significance of findings was evaluated by the Dunnett's test (one-sided); $^{*}P < 0.05$ and $^{**}P < 0.01$, compared with the vehicle group at each time point. (B) Maximum IOP reduction. Data are the mean mm Hg ± SE. The significance of findings was evaluated by the Williams' test (one-sided) $^{*}P < 0.05$; and by t-test (one-sided) $^{###}P < 0.001$, compared with the vehicle group. Baseline IOPs were 17.8 ± 0.2, 17.9 ± 0.2, 17.8 ± 0.4, 17.3 ± 0.2, and 17.5 ± 0.2 mm Hg (mean ± SE) with vehicle, 0.003%, 0.01%, 0.03%, and 0.05% Y-39983, respectively.

punctate subconjunctival hemorrhages were not observed in eyes treated with Y-39983, although conjunctival hyperemia was observed in eyes treated with Y-39983 in both species. To elucidate the mechanisms responsible for the punctate subconjunctival hemorrhages, we examined morphologic changes in cultured HUVECs after the addition of Y-39983. In medium containing 1 μM Y-39983, HUVECs exhibited contraction (Figs. 6A-C). The morphologic changes in HUVECs were reversible and had nearly recovered by 1 hour after removal of Y-39983 (Fig. 6D).

DISCUSSION

In the present study, topical administration of a selective inhibitor of the ROCK/ROK family of protein kinases, Y-39983, significantly reduced IOP in rabbit and monkey eyes. Several clinical investigations have revealed that elevated IOP is a major factor that causes glaucomatous optic neuropathy.[34-36] Because they potently lower IOP in mammalian eyes, ROCK inhibitors have been considered potential drugs for the treatment of glaucoma.[18,19] In this study, we examined the efficacy and safety of Y-39983 for potential clinical application.

Although our previous study revealed significant IOP-lowering effects of Y-27632 in animal eyes,[18,19] for potential clinical use, this compound has the disadvantage of poor stability in solution (data not shown). A series of modifications of molecular structure was therefore conducted to develop a more suitable form and more potent ROCK inhibitory activity for clinical use. Among the forms obtained, Y-39983 exhibits potent inhibition of ROCK activity and has acceptable stability, even in solution. Furthermore, we found that the ratio of IC_{50} for inhibition of ROCK/PKC for Y-39983 was 117 while that for Y-27632 was 82, suggesting that Y-39983 has the same specificity for ROCK as Y-27632. Also, the inhibition of ROCK by Y-39983 was 30 times that by Y-27632. These in vitro findings suggest that Y-39983 is a more useful candidate for an antiglaucoma drug than Y-27632. In our previous study,[18] Y-27632 at concentrations of 0.34% to 3.4% reduced IOP by 7 to 12 mm Hg in rabbit eyes under the same conditions of administration as in this study. Reduction of IOP (ΔIOP ≥ 10 mm Hg) was observed with a lower dose of Y-39983 (0.03%-0.1%). In addition, the degree of reduction of IOP (maximum ΔIOP = 5.3 mm Hg) obtained with 0.1% Y-27632, as determined in a previous study,[19] was observed with 0.01% Y-39983 (peak ΔIOP = 6.6 mm Hg). These findings together suggest that the reduction of IOP by Y-39983 is approximately 10-fold higher than that by Y-27632. These findings appear to agree with our in vitro result that the ROCK inhibitory activity of Y-39983 is 30 times that of Y-27632.

In considering clinical application of Y-39983, the next important question is whether Y-39983 is also effective in lowering IOP in primate eyes, since primate eyes have a modality of aqueous outflow different from that of lower mammalian eyes. The present study revealed that, even in monkey eyes, 0.05% Y-39983 induces significant IOP reduction almost equal to that obtained with 0.005% latanoprost. The IOP-lowering effect of Y-39983 in monkey eyes suggests the possibility of clinical use of this compound.

In this study, we examined the IOP-lowering effects of Y-39983 in rabbits and monkeys. With 0.05% Y-39983, maximum reductions of IOP were 12.1 ± 1.5 (mean ± SE) and 2.5 ± 0.2 mm Hg in rabbits and monkeys, respectively, showing that the magnitude of effect of Y-39983 in monkeys was much less than that in rabbits. This difference between species may be explained by the difference in baseline IOPs, which were 22.0 ± 0.6 and 17.5 ± 0.2 mm Hg in rabbits and monkeys, respectively. In fact, it has been reported that the IOP-lowering effects of H-7 and prostaglandin analogues in monkeys, which have low baseline IOPs, are weaker than that in rabbits, which have high baseline IOPs.[30,37] In a preliminary

TABLE 2. Effect of 0.05% of Y-39983 on Outflow Facility in Rabbit Eyes

	Outflow Facility (μL/min per mm Hg)	Uveoscleral Outflow (μL/min)
Y-39983	0.168 ± 0.018	0.470 ± 0.034
Vehicle	0.111 ± 0.014	0.478 ± 0.031
Significance	$P < 0.001$	NS
% Change	+65.5%	−0.9%

Data are the mean ± SE (n = 10). Significance was evaluated by paired t-test (one-sided).

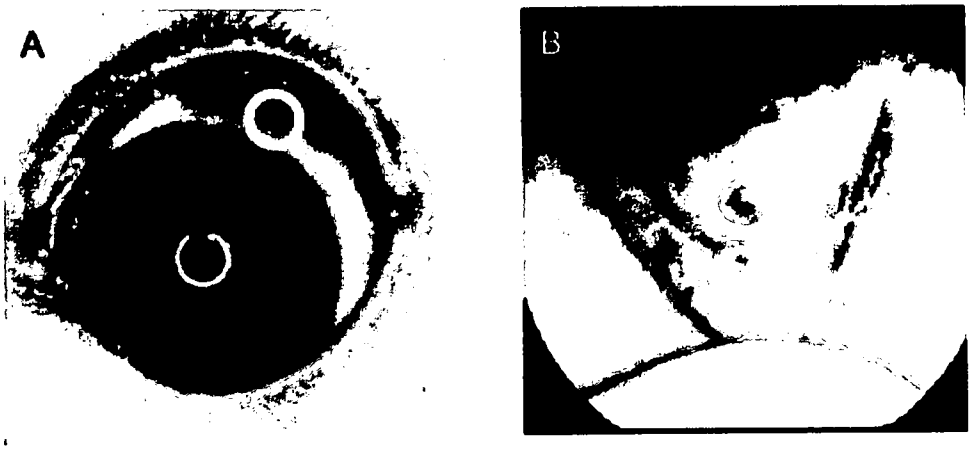

FIGURE 5. Examples of subconjunctival hemorrhage in rabbit and monkey eyes. Y-39983 was topically administered to eyes four times a day (at 2-hour intervals) for 4 and 26 weeks in rabbits and monkeys, respectively. (A) A rabbit eye treated with 0.03% Y-39983. (B) A monkey eye treated with 0.03% Y-39983.

pharmacokinetics study after topical administration of Y-39983, the disappearance of Y-39983 in tears of monkeys was faster than that in rabbits, and this difference in pharmacokinetics may be due to differences in frequency of blinking in these species. This difference in pharmacokinetics may also have resulted in the difference in IOP-lowering effects in rabbits and monkeys in this study.

There are two routes of aqueous humor outflow: that via the conventional (trabecular) and that via the unconventional (uveoscleral) pathway.[20] In primate and human eyes, conventional outflow is considered the main route and is believed to be regulated by the cellular behavior and contractility of TM cells.[38,39] Our previous study showed that Y-27632 increased conventional outflow by altering the contractility of TM cells.[18] In addition, Y-27632 has been shown to increase conventional outflow by inducing cellular relaxation and loss of cell-substratum adhesion in the TM and in SC cells.[23] Our outflow measurements suggest that Y-39983 may also affect the contractility of TM and SC cells, resulting in increased conventional outflow. Consistent with this, it has been demonstrated that TM exhibits higher levels of mRNA for ROCK and ROCK substrates than CM in human and monkey eyes, suggesting that TM is one of the major sites of regulation of IOP by ROCK.[25]

The IOP-lowering mechanism of H-7, a broad-spectrum inhibitor of serine-threonine kinases including ROCK, has been investigated.[27,28,30] H-7 also increases conventional outflow by altering the shape, actin cytoskeleton, and cell-cell adhesion of TM and SC cells, as Y-27632. Thus, alterations of TM and SC cells affect conventional outflow, and compounds causing cytoskeletal change in TM and SC cells may potentially be useful as antiglaucoma drugs.

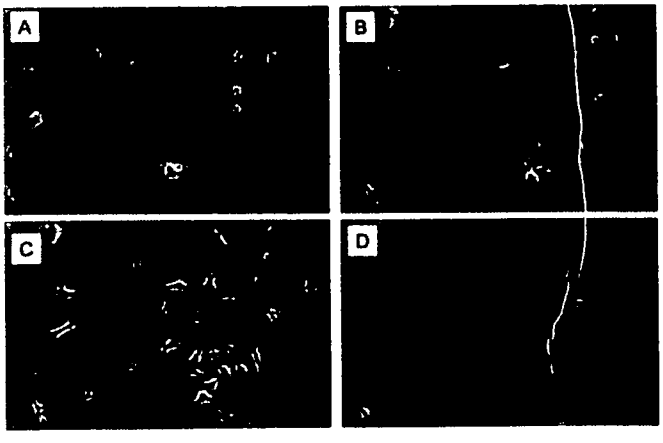

FIGURE 6. Effects of Y-39983 on morphology of HUVECs. Phase-contrast microscopic observation of HUVECs in the same region. (A) Nontreatment or (B) treatment with 1 μM Y-39983 for 15 minutes or (C) for 30 minutes. *Arrows*: contracted cells. (D) Replacement with medium without Y-39983 for 1 hour.

In our toxicologic study, no serious side effects were observed in ocular tissues of rabbits and monkeys except sporadic punctate subconjunctival hemorrhage. This type of hemorrhage was observed after frequent administration of Y-39983 (four times a day at 2-hour intervals). The side effects may be explained by impairment of barrier function or morphologic changes in vascular endothelial cells, as shown in the experiments using HUVECs. The morphologic changes in HUVECs observed after the addition of Y-39983 suggest the possibility of impairment of barrier function in vascular endothelial cells in the retina, since the Rho-ROCK signaling pathway is considered ubiquitous. However, our animal experiments did not reveal detectable hemorrhages in the iris-ciliary body or retina-choroid, suggesting that the concentration at which lowering of IOP is elicited may not be high enough to induce hemorrhage in the ocular fundus. Also, subconjunctival hemorrhage, which was encountered with frequent administration (four times a day), was not observed with administration two or three times a day. It is possible that no side effects will be induced in the conjunctiva with clinical usage of Y-39983, if excessively frequent instillation is avoided.

In summary, the present study showed that Y-39983, a selective and potent ROCK inhibitor, reduced IOP and increased aqueous outflow. Selective inhibition of the Rho/ROCK signaling pathway may be a useful new strategy for the treatment of glaucoma, and Y-39983 ophthalmic solution may be a candidate drug since it lowers IOP by increasing aqueous conventional outflow and produces fewer side effects.

References

1. Nobes C, Hall A. Regulation and function of the Rho subfamily of small GTPases. *Curr Opin Genet Dev.* 1994;4:77-81.
2. Takai Y, Sasaki T, Tanaka K, Nakanishi H. Rho as a regulator of the cytoskeleton. *Trends Biochem Sci.* 1995;20:227-231.
3. Ridley AJ, Paterson HF, Johnston CL, Diekmann D, Hall A. The small GTP-binding protein rac regulates growth factor-induced membrane ruffling. *Cell.* 1992;70:401-410.
4. Ridley AJ, Hall A. Signal transduction pathways regulating Rho-mediated stress fiber formation: requirement for a tyrosine kinase. *EMBO J.* 1994;13:2600-2610.
5. Narumiya S. The small GTPase Rho: cellular functions and signal transduction. *J Biochem (Tokyo).* 1996;120:215-228.
6. Narumiya S, Ishizaki T, Watanabe N. Rho effector and reorganization of actin cytoskeleton. *FEBS Lett.* 1997;410:68-72.

7. Paterson HF, Self AJ, Garrett MD, Just I, Aktories K, Hall A. Microinjection of recombinant p21rho induces rapid changes in cell morphology. *J Cell Biol.* 1990;111:1001-1007.
8. Takaishi K, Sasaki T, Kato M, et al. Involvement of Rho p21 small GTP-binding protein and its regulator in the HGF-induced cell motility. *Oncogene.* 1994;9:273-279.
9. Kishi K, Sasaki T, Kuroda S, Itoh T, Takai Y. Regulation of cytoplasmic division of *Xenopus* embryo by rho p21 and its inhibitory GDP/GTP exchange protein (rho GDI). *J Cell Biol.* 1993;120:1187-1195.
10. Hirata K, Kikuchi A, Sasaki T, et al. Involvement of rho p21 in the GTP-enhanced calcium ion sensitivity of smooth muscle contraction. *J Biol Chem.* 1992;267:8719-8722.
11. Gong MC, Iizuka K, Nixon G, et al. Role of guanidine nucleotide-binding proteins—ras-family or trimeric proteins or both—in Ca^{2+} sensitization of smooth muscle. *Proc Natl Acad Sci USA.* 1996;93:1340-1345.
12. Ishizaki T, Naito M, Fujisawa K, et al. p160ROCK, a Rho-associated coiled-coil forming protein kinase, works downstream of Rho and induces focal adhesions. *FEBS Lett.* 1997;404:118-124.
13. Nakagawa O, Fujisawa K, Ishizaki T, Saito Y, Nakao K, Narumiya S. ROCK-I and ROCK II, two isoforms of Rho-associated coiled coil forming protein serine/threonine kinase in mice. *FEBS Lett.* 1996;392:189-193.
14. Leung T, Chen XQ, Manser E, Lim L. The p160 RhoA-binding kinase ROK alpha is a member of a kinase family and is involved in the reorganization of the cytoskeleton. *Mol Cell Biol.* 1996;16:5313-5327.
15. Matsui T, Amano M, Yamamoto T, et al. Rho-associated kinase, a novel serine/threonine kinase, as a putative target for small GTP binding protein Rho. *EMBO J.* 1996;15:2208-2216.
16. Amano M, Chihara K, Kimura K, et al. Formation of actin stress fibers and focal adhesions enhanced by Rho-kinase. *Sctence.* 1997;275:1308-1311.
17. Uehata M, Ishizaki T, Satoh H, et al. Calcium sensitization of smooth muscle mediated by a Rho-associated protein kinase in hypertension. *Nature.* 1997;389:990-994.
18. Honjo M, Tanihara H, Inatani M, et al. Effects of rho-associated protein kinase inhibitor Y-27632 on intraocular pressure and outflow facility. *Invest Ophthalmol Vis Sci.* 2001;42:137-144.
19. Waki M, Yoshida Y, Oka T, Azuma M. Reduction of intraocular pressure by topical administration of an inhibitor of the Rho-associated protein kinase. *Curr Eye Res.* 2001;22:470-474.
20. Kaufman PL. Pressure-dependent outflow. In: Hart WM, ed. *Alder's Physiology of the Eye: Clinical Application.* 9th ed. St. Louis: Mosby;1992;307-335.
21. Epstein DL, Rohen JW. Morphology of the trabecular meshwork and inner-wall endothelium after cationized ferritin perfusion in the monkey eye. *Invest Ophthalmol Vis Sci.* 1991;32:160-171.
22. Tian B, Geiger B, Epstein DL, Kaufman PL. Cytoskeletal involvement in the regulation of aqueous humor flow. *Invest Ophthalmol Vis Sci.* 2000;41:619-623.
23. Rao PV, Deng PF, Kumar J, Epstein DL. Modulation of aqueous humor outflow facility by the Rho kinase-specific inhibitor Y-27632. *Invest Ophthalmol Vis Sci.* 2001;42:1029-1037.
24. Mettu PS, Deng PF, Misra UK, Gawdi G, Epstein DL, Rao PV. Role of lysophospholipid growth factors in the modulation of aqueous humor outflow facility. *Invest Ophthalmol Vis Sci.* 2004;45:2263-2271.
25. Nakajima E, Nakajima T, Minagawa Y, Shearer TS, Azuma M. Contribution of ROCK in contraction of trabecular meshwork: proposed mechanism for regulating aqueous outflow in monkey and human eyes. *J Pharm Sci.* 2005;94:701-708.
26. Rosenthal R, Choritz L, Schlott S, et al. Effects of ML-7 and Y-27632 on carbachol- and endothelin-1-induced contraction of bovine trabecular meshwork. *Exp Eye Res.* 2005;80:837-845.
27. Tian B, Kaufman PL, Volberg T, Gablet BT, Geiger B. H-7 disrupts the actin cytoskeleton and increases outflow facility. *Arch Ophthalmol.* 1998;116:633-643.
28. Liu X, Cai S, Glasser A, et al. Effect of H-7 on cultured human trabecular meshwork cells. *Mol Viston.* 2001;7:145-153.
29. Honjo M, Inatani M, Kido N, et al. Effects of protein kinase inhibitor, HA1077, on intraocular pressure and outflow facility in rabbit eyes. *Arch Ophthalmol.* 2001;119:1171-1178.
30. Tian B, Wang RF, Podos SM, Kaufman PL. Effects of topical H-7 on outflow facility, intraocular pressure, and corneal thickness in monkeys. *Arch Ophthalmol.* 2004;122:1171-1177.
31. Bárány EH. Simultaneous measurement of changing intraocular pressure and outflow facility in the vervet monkey by constant pressure perfusion. *Invest Ophthalmol Vis Sci.* 1964;3:135-143.
32. Taniguchi T, Haque MS, Sugiyama K, Hori N, Kitazawa Y. Ocular hypotensive mechanism of topical isopropyl unoprostone, a novel prostaglandin metabolite-related drug, in rabbits. *J Ocul Pharmacol Ther.* 1996;12:489-498.
33. Bill A. The aqueous humor drainage mechanism in the cynomolgus monkey (Macaca irus) with evidence for unconventional routes. *Invest Ophthalmol Vis Sci.* 1965;4:911-919.
34. Gordon MO, Beiser JA, Brandt JD, et al. The Ocular Hypertension Treatment Study: baseline factors that predict the onset of primary open-angle glaucoma. *Arch Ophthalmol.* 2002;120:714-720, discussion 829-830.
35. Leske MC, Heijl A, Hussein M, Bengtsson B, Hyman L, Komaroff E. Early Manifest Glaucoma Trial Group. Factors for glaucoma progression and the effect of treatment: the early manifest glaucoma trial. *Arch Ophthalmol.* 2003;121:48-56.
36. Nouri-Mahdavi K, Hoffman D, Coleman AL, et al. Advanced Glaucoma Intervention Study. Predictive factors for glaucomatous visual field progression in the Advanced Glaucoma Intervention Study. *Ophthalmology.* 2004;111:1627-1635.
37. Serle JB, Podos SM, Kitazawa Y, Wang RF. A comparative study of latanoprost (Xalatan) and isopropyl unoprostone (Rescula) in normal and glaucomatous monkey eyes. *Jpn J Ophthalmol.* 1998;42:95-100.
38. Yue BY, Higginbotham EJ, Chang IL. Ascorbic acid modulates the production of fibronectin and laminin by cells from an eye tissue-trabecular meshwork. *Exp Cell Res.* 1990;187:65-68.
39. Sawaguchi S, Yue BY, Chang IL, Wong F, Higginbotham EJ. Ascorbic acid modulates collagen type I gene expression by cells from an eye tissue-trabecular meshwork. *Cell Mol Biol.* 1992;38:587-604.

Available online at www.sciencedirect.com
ScienceDirect
Experimental Eye Research 84 (2007) 1074–1080
EXPERIMENTAL EYE RESEARCH
www.elsevier.com/locate/yexer

Effect of pitavastatin on experimental choroidal neovascularization in rats☆

Nina Sagara, Takahiro Kawaji*, Akiomi Takano, Yasuya Inomata, Masaru Inatani, Mikiko Fukushima, Hidenobu Tanihara

Department of Ophthalmology and Visual Science, Graduate School of Medical Sciences, Kumamoto University, 1-1-1 Honjo, Kumamoto 860-8556, Japan

Received 14 September 2006; accepted in revised form 1 February 2007
Available online 11 February 2007

Abstract

The association between the use of statins and age-related macular degeneration (AMD), a leading cause of blindness, has been evaluated in many clinical studies; however, the results have been contradictory. We evaluated the effect of pitavastatin administration on laser-induced experimental choroidal neovascularization (CNV) in rats. Brown Norway rats received pitavastatin (1.0 mg/kg per day) for 1 day prior to laser-induced CNV and continued to receive the drug for 14 days. Fluorescein angiograms were graded by masked observers. CNV area and thickness were assessed by fluorescein isothiocyanate-labeled dextran angiography and histology, respectively. Vascular endothelial growth factor (VEGF), monocyte chemoattractant protein-1 (Ccl-2; also known as MCP-1), and intercellular adhesion molecule-1 (ICAM-1) mRNA levels were measured using reverse-transcription polymerase chain reaction (RT-PCR) and real-time quantitative RT-PCR. Pitavastatin-treated rats had significantly less fluorescence leakage compared with the vehicle-treated rats estimated by CNV score using fluorescein angiography. Both the area and the thickness of CNV in pitavastatin-treated rats were significantly reduced compared with the vehicle-treated rats. Gene expression of VEGF, Ccl-2, and ICAM-1 were significantly decreased by pitavastatin administration in experimental CNV. Thus, we demonstrated that the therapeutic dose of pitavastatin for human hypocholesterolemia effectively suppressed experimental CNV in rats. The use of pitavastatin may be helpful in preventing CNV development in AMD patients.

Keywords: choroidal neovascularization; HMG-CoA reductase inhibitor; pitavastatin; age-related macular degeneration

1. Introduction

The exudative form of age-related macular degeneration (AMD) is the major cause of visual loss in well-developed countries (Fine et al., 2000). The main pathological change of the exudative form of AMD is choroidal neovascularization (CNV). An essential element in the growth of CNV is the rupture of Bruch's membrane and the proliferation of blood vessels through breaks in the membrane. However, the pathogenesis of CNV is not completely understood (Zarbin, 2004).

In recent years, statins, the 3-hydroxy-3-methylglutaryl coenzyme A (HMG-CoA) reductase inhibitors, have been widely used in the treatment of atherosclerotic diseases and hyperlipidemia (Mahley et al., 1999; Vaughan et al., 2000). In addition to their lipid-lowering properties, statins have been thought to exert an expanded profile of non-lipid-related pleiotropic effects, including improved endothelial function and decreased low-density lipoprotein oxidation, foam cell formation, leukocyte–endothelium interactions, plaque rupture, and smooth muscle cell proliferation (Bellosta et al., 2000; Hess and Fagan, 2001; Takemoto and Liao, 2001). Furthermore, statins have been found to exert both anti-inflammatory and anti-angiogenic effects, which are relevant to vascular disease and may also be relevant in the pathogenesis of AMD (Pruefer

☆ Supported in part by a Grant-in-Aid for Scientific Research from the Ministry of Education, Science, Sports and Culture, Japan from the Ministry of Health and Welfare, Japan.
* Corresponding author. Tel.: +81 96 373 5247; fax: +81 96 373 5249.
E-mail address: kawag@white.plala.or.jp (T. Kawaji).

0014-4835/$ - see front matter © 2007 Elsevier Ltd. All rights reserved.
doi:10.1016/j.exer.2007.02.005

et al., 1999; Jialal et al., 2001; Kwak et al., 2001). These lipid- and non-lipid-related effects are considered to be protective against cardiovascular diseases (Plenge et al., 2002; Wassmann et al., 2003).

Recently, many extensive epidemiological studies have demonstrated that AMD shares a number of overlapping risk factors with atherosclerosis, including age, cigarette smoking, hypertension, obesity, and increased dietary fat intake (Mitchell et al., 1995; Klaver et al., 2001; McCarty et al., 2001; Mitchell et al., 2002). Considering their well-established effectiveness in cardiovascular disease, statins may also be effective in the management of AMD. In recent years, a small cross-sectional survey suggested that statins exert a protective effect in AMD (Hall et al., 2001). However, subsequent studies have produced inconsistent results (McCarty et al., 2001; McGwin et al., 2003; Klein et al., 2003; Wilson et al., 2004; McGwin et al., 2006).

In this study, we evaluated the effect of the administration of pitavastatin (so-called vascular statin), which has a high affinity for vascular endothelium, on experimental CNV created by laser-induced rupture of Bruch's membrane, which stimulates preexisting capillaries to proliferate into new capillary networks, in rats. The murine model of experimental CNV was used because rats are resistant to the hypocholesterolemic effect of statins.

2. Materials and methods

2.1. Experimental CNV model in rats

Six-week-old male Brown Norway (BN) rats (Seac Yoshitomi, Fukuoka, Japan) weighing 120–160 g were used. The animals were handled in accordance with institutional guidelines and the ARVO Statement for the Use of Animals in Ophthalmic and Vision Research. The BN rats were anesthetized by intramuscular injection of a 1 mL/kg mixture (1:1) of ketamine hydrochloride (Ketalar; Sankyo, Tokyo, Japan) and xylazine hydrochloride (Celactal; Bayer, Tokyo, Japan), and their pupils were dilated with tropicamide (0.5% Mydrin M; Santen Pharmaceutical, Osaka, Japan). Experimental CNV was created as described previously (Takehana et al., 1999). Briefly, four laser photocoagulations were applied to each eye between the major retinal vessels around the optic disk under the following conditions: power 150 mW, wavelength 521 nm, duration 100 ms and spot size 100 μm. Bruch's membrane was breached, as evidenced clinically by central bubble formation, without intraretinal or choroidal hemorrhage.

2.2. Drug administration

The total 38 BN rats were divided into two groups: pitavastatin-treated ($n = 19$) and vehicle-treated ($n = 19$). Pitavastatin (Livalo, previously known as NK-104) was kindly provided by Kowa (Tokyo, Japan). It was dissolved in 0.5% carboxymethylcellulose (CMC) sodium salt (Wako, Osaka, Japan) and administered at a dose of 1 mg kg^{-1} day^{-1} (pitavastatin-treated rats). Control rats (vehicle-treated rats) received 0.5% CMC vehicle. Oral gavage was performed with a 20-gauge blunt feeding needle for 1 day prior to the laser induction of CNV and continued daily until the rats were killed and evaluated.

2.3. Fluorescein angiography

At day 14 after laser induction of CNV, the laser lesions were studied by fluorescein angiography to evaluate CNV development and its activity. Each rat was injected with 0.5 ml of 10% fluorescein sodium (Fluorescite; Alcon, Tokyo, Japan) intraperitoneally, and fundus angiogram photographs were taken at early and late phases using a scanning laser ophthalmoscope (SLO101; Rodenstock, Germany). The formation of CNV was evaluated according to the size and the presence or absence of dye leakage, as described previously (Takehana et al., 1999; Tanemura et al., 2004). The guideline for CNV scoring was as follows: no leakage (score 0); minimum leakage or a staining of tissue with no leakage (score 1); small but evident leakage less than 1/4 disc area (score 2); large evident leakage (score 3). A typical photograph of each CNV score is shown in Fig. 1. Two examiners judged the scores in a masked fashion. When the two scores given for a particular lesion did not coincide, the higher score was used for the analysis.

2.4. FITC-dextran angiogrphy

Fluorescein isothiocyanate (FITC)-dextran angiography was performed on the rats 14 days after laser induction of CNV by the method described previously (Edelman and Castro, 2000; Semkova et al., 2003), with slight modifications. The rats were deeply anesthetized and perfused with 50 mL phosphate buffered saline (PBS) with 5 mg/mL FITC-labeled dextran (MW 2×10^6; Sigma, St Louis, MO, USA) via the left ventricle through a 12-gauge cannula. The animals were sacrificed, and the eyes were enucleated and fixed in 4% paraformaldehyde for 5 h. Retinal pigment epithelium (RPE)-choroid-sclera flat mounts were obtained by hemisecting the eye and peeling the neural retina away from the eyecup. The flat mounts were laid flat onto a microscope slide with the RPE facing up. All flat mounts described here and later were examined with a fluorescence microscope (BX51; OLYMPUS, Tokyo, Japan) using FITC filters. The images of the laser lesions (= CNV area) were measured with computer-assisted image-analysis software (Lumina Vision; Mitani Corporation, Fukui, Japan).

2.5. Histopathologic studies

Histopathologic studies were performed on eyes from pitavastatin-treated rats and vehicle-treated rats at day 14 after laser induction of CNV. The rats were killed with an overdose of sodium pentobarbital. The eyes were enucleated and immersed overnight in PBS containing 2.5% glutaraldehyde and 4% paraformaldehyde. The retina-choroid-sclera were dehydrated and embedded in paraffin. Serial sections of 6-μm thickness were cut to determine the center of each lesion and stained

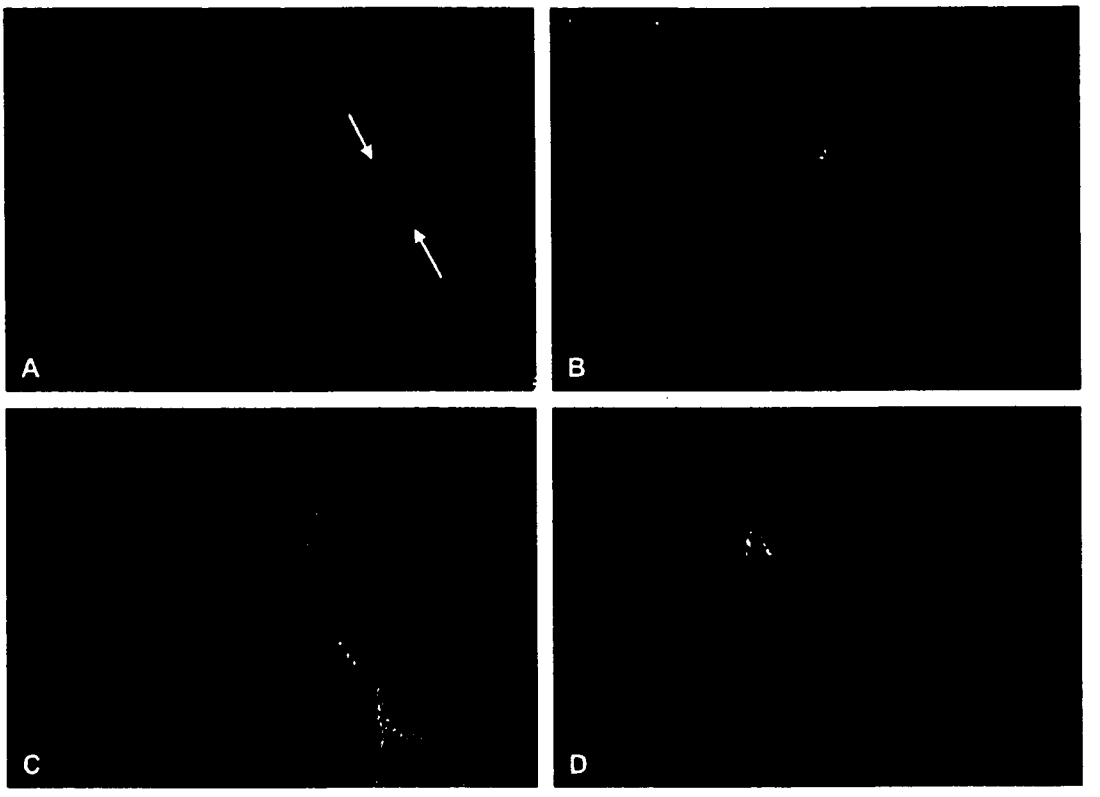

Fig. 1. Typical examples of each CNV score in the fluorescein angiogram after laser-induced CNV in rat retina. Each laser spot was scored from 0 to 3 according to the size and the presence or absence of dye leakage on the early and late phase angiogram photographs. The guideline for the CNV scoring was as follows: (A) no leakage (score 0); (B) minimum leakage or a staining of tissue with no leakage (score 1); (C) small but evident leakage less than 1/4 disc area (score 2); (D) large evident leakage (score 3).

with hematoxylin and eosin (H&E) for light microscopy. Subsequent measurements were performed by examining stained sections under a microscope (BX51; OLYMPUS, Tokyo, Japan). The maximum CNV thickness, from the bottom of the pigmented choroidal layer to the top of the neovascular membrane, was measured using the middle section of each lesion of each eye.

2.6. RT-PCR and real-time quantitative RT-PCR

Five eyes from five rats each in the vehicle-treated and pitavastatin-treated groups were obtained to evaluate the angiogenic and inflammatory mechanism in the laser-induced CNV model, including the mRNA levels of vascular endothelial growth factor (VEGF), monocyte chemoattractant protein-1 (Ccl-2; also known as MCP-1) and intercellular adhesion molecule-1 (ICAM-1). Total RNA was isolated from the retina-RPE-choroid-sclera 3 days after laser photocoagulation using the SV Total RNA Isolation System (Promega, Madison, WI, USA) according to the manufacturer's protocol. To remove genomic DNA, the total RNA preparation was treated with DNase I (Promega, Tokyo, Japan). Reverse-transcription polymerase chain reaction (RT-PCR) was performed with 10 ng of total RNA on a 9800 Fast Thermal Cycler (Applied Biosystems, Foster City, CA, USA) using the SuperScript One-Step RT-PCR with Platinum Taq (Invitrogen, Carlsbad, CA, USA) and Taqman Gene Expression assays (Applied Biosystems) to check expression of mRNAs for rat VEGF, Ccl-2, ICAM-1 and actin beta (Actb). The assay IDs are as follows: VEGF assay ID, Rn 00582395_ m1; Ccl-2 assay ID, Rn 00580555_m1; ICAM-1 Assay ID, Rn 005642227_ m1: and Actb Assay ID, Rn00667869_m1. Although these sequences of commercially available primers were undocumented, these primers were designed for spanning between exon 2 and exon 3 so that cDNA fragments were easily distinguishable from genomic fragments. Total RNA was reverse transcribed into cDNA by one cycle at 50 °C for 30 min and one cycle at 95 °C for 10 min. The cDNA was amplified for 40 cycles at 95 °C for 15 s and 60 °C for 1 min. Ten micro liter samples of these PCR products were applied to a 3% agarose gel, electrophoresed, stained with ethidium bromide, and photographed.

In addition, real-time quantitative RT-PCR was performed with 10 ng of total RNA on an ABI Prism 7000 Sequence Detection System (Applied Biosystems) using the SuperScript One-Step RT-PCR with Platinum Taq and Taqman Gene Expression assays, to quantify the mRNAs for rat VEGF, Ccl-2, ICAM-1, and Actb. Total RNA was reverse transcribed into cDNA under the same conditions as the RT-PCR. The cDNA was amplified for 50 cycles at 95 °C for 15 s and 60 °C for 1 min. Specificity of amplification products was confirmed by conducting a melting curve of the samples after each run. The threshold cycle of fluorescence units was evaluated to quantify the amount of each mRNA. VEGF, Ccl-2, and ICAM-1 mRNA levels were normalized by the Actb mRNA level.

2.7. Statistical analysis

All results are expressed as mean ± standard error (SE). The statistical significance of CNV score, CNV area, and CNV thickness was determined using an unpaired *t*-test. VEGF, Ccl-2, and ICAM-1 mRNA levels were statistically analyzed using the Mann–Whitney *U*-test. *P* values less than 0.05 were considered statistically significant.

3. Results

3.1. Fluorescein angiography

Laser spots in each vehicle-treated rat ($n = 8$) and pitavastatin-treated rat ($n = 8$) were applied and scored as follows: score 0, 1 spot, 5 spots; score 1, 14 spots, 22 spots; score 2, 19 spots, 18 spots; score 3, 11 spots, 0 spot (Fig. 2A). As shown in Fig. 2B, the mean CNV scores in pitavastatin-treated and vehicle-treated rats were 1.29 ± 0.09 and 1.89 ± 0.12, respectively. There was a statistically significant difference between these two groups ($P < 0.05$, unpaired *t*-test).

3.2. FITC-dextran angiogrphy

In the current study, FITC-dextran was used to label the blood vessel lumen, and RPE-choroid-sclera flat mounts were examined by fluorescence microscopy to follow experimental CNV 14 days after laser photocoagulation. Fig. 3A,B show fluorescent images of CNV in laser lesions in RPE-choroid-sclera flat mounts from vehicle-treated (3A) and pitavastatin-treated (3B) rats. CNV appeared as a network of broad, flat microvessels, reminiscent of choriocapillaries that spanned a circular area approximately 300 μm in diameter. The mean CNV area in pitavastatin-treated rats ($n = 11$, $29.5 \pm 2.85 \times 10^3$ μm^2) was significantly smaller than that in vehicle-treated rats ($n = 11$, $41.2 \pm 2.48 \times 10^3$ μm^2) ($P < 0.05$, unpaired *t*-test) (Fig. 3C).

3.3. Histopathologic studies

Fig. 4A,B show representative H&E-stained sections from CNV lesions 14 days after laser photocoagulation. In the laser lesions, multilayered fusiform proliferative membranes were seen in the central area of the lesion underlying the RPE to the choroid, and blood vessels with red blood cells were also seen. The thickness of CNV lesions in pitavastatin-treated rats ($n = 3$, 73.4 ± 15.4 μm) was significantly thinner than that in vehicle-treated rats ($n = 3$, 114.2 ± 8.1 μm) ($P < 0.05$, unpaired *t*-test) (Fig. 4C).

3.4. RT-PCR and real-time quantitative RT-PCR

To investigate the mechanism of the inhibitory effect of pitavastatin on experimental CNV, we performed RT-PCR and real-time quantitative RT-PCR (Fig. 5). RT-PCR revealed that VEGF, Ccl-2, and ICAM-1 mRNA levels in pitavastatin-treated rats were lower than those in vehicle-treated rats (Fig. 5A). Furthermore, real-time quantitative RT-PCR analysis revealed that VEGF, Ccl-2, and ICAM-1 mRNA levels in pitavastatin-treated rats were significantly lower than those in vehicle-treated rats ($P < 0.05$, Mann–Whitney *U*-test) (Fig. 5B–D). The expression rate of Actb almost unchanged in pitavastatin-treated rats similar to vehicle-treated rats.

4. Discussion

In the present study, we demonstrated that the therapeutic dose of pitavastatin for human hypocholesterolemia effectively suppressed experimental CNV in rats. The pitavastatin-treated group had significantly less fluorescence leakage compared with the vehicle-treated group on fluorescein angiography. The area of CNV measured by FITC-dextran angiogrphy in the pitavastatin-treated group was also significantly smaller than that in the vehicle-treated group. In addition, through histopathologic studies we showed that

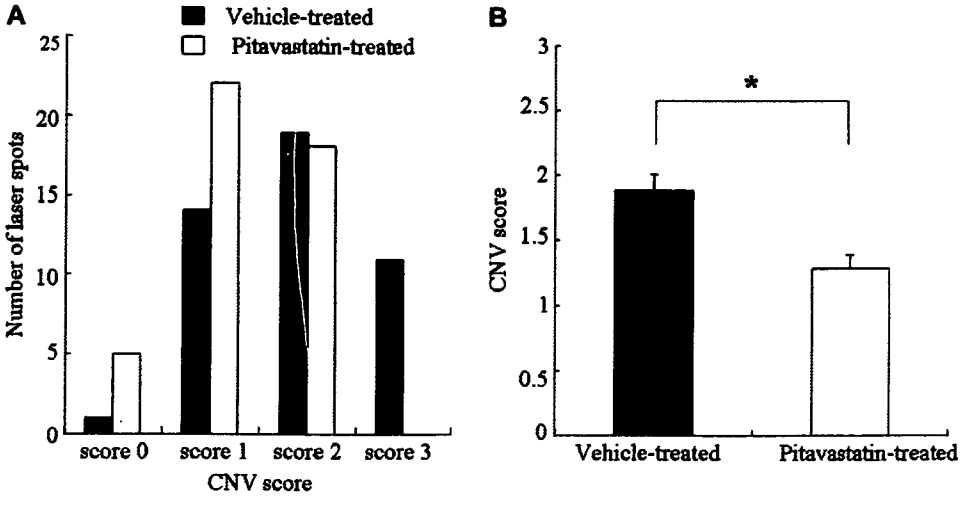

Fig. 2. Effect of pitavastatin on CNV score 14 days after laser-induced CNV in rat retina. Number of laser lesions of each 0–3 CNV scores in vehicle-treated and pitavastatin-treated rats (A). The mean CNV score in vehicle-treated and pitavastatin-treated rats (B). *, $P < 0.05$ compared with vehicle-treated.

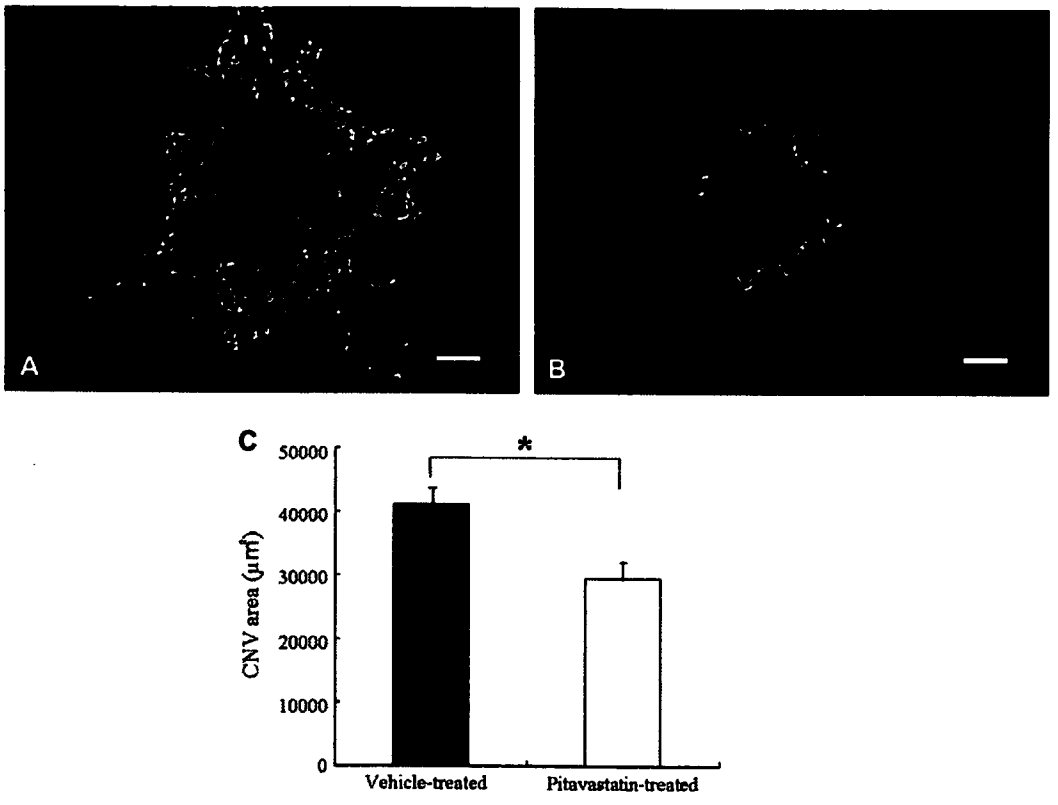

Fig. 3. Effect of pitavastatin on CNV area 14 days after laser-induced CNV in rat retina. CNV is described with green fluorescence by FITC-dextran angiography in vehicle-treated rats (A) and in pitavastatin-treated rats (B). Computer image analysis of CNV area in pitavastatin-treated rats was significantly smaller than the area in vehicle-treated rats (C). Scale bar = 100 μm (A and B). *, $P < 0.05$ compared with vehicle-treated.

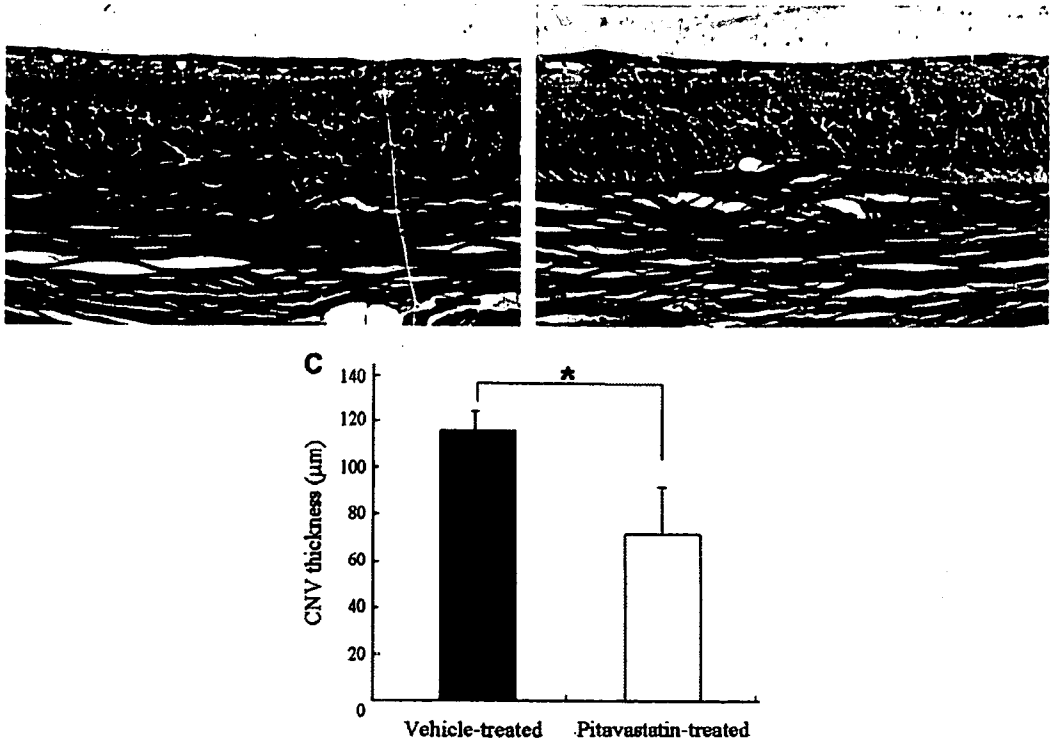

Fig. 4. Effect of pitavastatin on CNV thickness 14 days after laser-induced CNV in rat retina. Light micrographs of Hematoxylin and Eosin stained sections of the CNV lesions in vehicle-treated rats (A) and pitavastatin-treated rats (B) 14 days after laser photocoagulations. Computer image analysis of CNV thickness in pitavastatin-treated rats was significantly thinner than that in vehicle-treated rats (C). Scale bar = 100 μm (A and B). *, $P < 0.05$ compared with vehicle-treated.

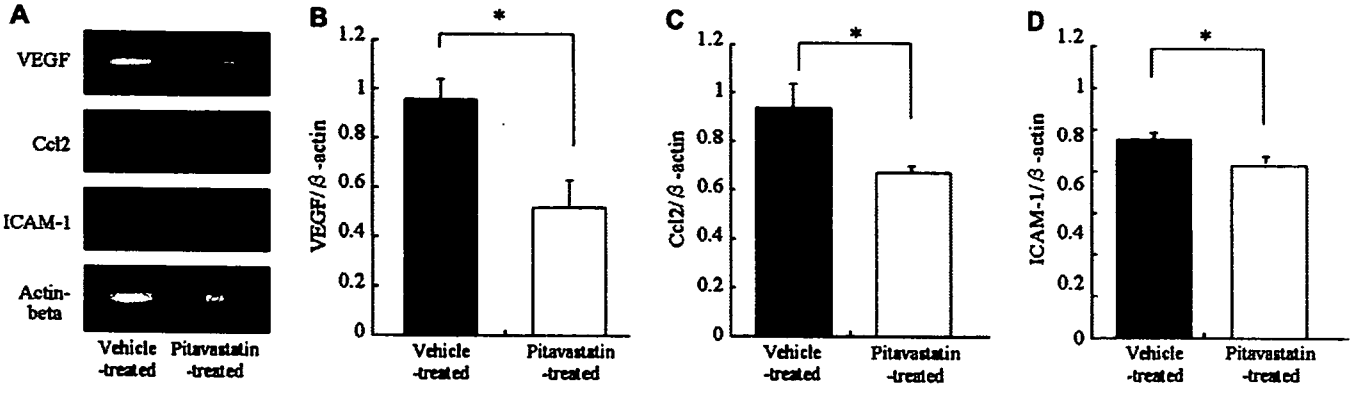

Fig. 5. Effect of pitavastatin on expression of VEGF, Ccl-2, and ICAM-1 mRNA 3 days after laser-induced CNV. RT-PCR analysis showed that VEGF, Ccl-2, and ICAM-1 mRNA expressions in pitavastatin-treated rats were lower than those in vehicle-treated rats (A). Real-time quantitative RT-PCR analysis revealed that VEGF, Ccl-2, and ICAM-1 mRNA levels in pitavastatin-treated rats were significantly decreased than those in vehicle-treated rats (B,C and D). *, $P < 0.05$ compared with vehicle-treated.

the CNV lesions in pitavastatin-treated rats were thinner than those in vehicle-treated rats. These data suggest that pitavastatin reduced the formation and development of experimental CNV. Furthermore, we present the first in vivo evidence that gene expression of VEGF, Ccl-2, and ICAM-1, which are important factors in the pathogenesis of AMD, was significantly decreased, suggesting that part of the mechanism of experimental CNV in rats is independent of the cholesterol-lowering effects of pitavastatin.

The etiology of AMD is obscure and the pathogenic pathways mediating the development of CNV are not understood. AMD and atherosclerosis have been shown to share a number of risk factors (Delcourt et al., 2001), leading to suggestions that they may have similar etiologies. The association between the use of statins and AMD has been evaluated in many clinical studies; however, the results have been contradictory (Hall et al., 2001; McCarty et al., 2001; McGwin et al., 2003; Klein et al., 2003; Wilson et al., 2004; McGwin et al., 2006). Moreover, the known pharmacodynamics of statins, such as their anti-inflammatory and anti-angiogenic effects, raises some possible mechanisms through which they may exert a protective effect in AMD.

Expression of VEGF has been demonstrated in surgically removed CNV tissues (Kvanta et al., 1996; Lopez et al., 1996) and in experimental CNV (Yi et al., 1997; Shen et al., 1998). It is well known that VEGF is the major stimulator in angiogenesis and has been shown to be correlated with the amount of inflammatory cells in CNV from AMD patients (Kvanta et al., 1996). The available in vitro data suggest that statins promote angiogenesis at lower doses, while under certain conditions some statins have the opposite effect (Urbich et al., 2002; Weis et al., 2002; Frick et al., 2003). Recently, it has been reported that therapeutic doses of pitavastatin reduced the incidence of CNV formation, but on increasing the dosage by 100-fold may exacerbate CNV leakage in experimental CNV in mice. However, retinal VEGF lysate levels did not mirror the changes in fluorescein leakage and CNV area on histological examination, suggesting a VEGF-independent mechanism for the statin effect (Zambarakji et al., 2006). In addition, we showed that therapeutic doses of pitavastatin not only reduced the incidence of CNV formation in rats but also suppressed VEGF gene expression, although we did not measure the retinal VEGF protein levels. VEGF synthesis has been shown to depend on the conditions under investigation, and the effects on VEGF were not paralleled by the angiogenic activity of endothelial cells (Frick et al., 2003).

It is well known that macrophages may play a role in the pathogenesis of AMD. Ccl-2 (also known as MCP1) is one of the most potent macrophage-recruiting molecules and is considered to be associated with the progression of CNV (Grossniklaus et al., 2002; Ambati et al., 2003). In addition, ICAM-1, which is involved in leukocyte endothelial adhesion and leukocyte migration through its receptor lymphocyte function associated antigen-1 (Mesri et al., 1994), has been proposed to be involved in the experimental CNV model (Shen et al., 1998; Sakurai et al., 2003). It has been reported that statins inhibit the expression in vitro and in vivo production of Ccl-2 (Romano et al., 2000), and leukocyte–endothelial interaction by blocking P-selectin and ICAM-1 in an ischemia-reperfusion injury model (Honjo et al., 2002). In this study, we demonstrated that pitavastatin effectively reduces gene expression of VEGF, Ccl-2, and ICAM-1 in an experimental CNV model in rats. Although we did not fully study the complex molecular mechanisms of the observed effect of pitavastatin on experimental CNV, it is possible that pitavastatin may attenuate experimental CNV development in rats through both anti-angiogenic and anti-inflammatory effects, independent of the lipid-lowering effect. Furthermore, pitavastatin (so-called vascular statin) has a high affinity for vascular endothelium. This high affinity might have had an effective on the experimental CNV.

Current treatment options for AMD are limited and to date have had little impact on the rate of blindness. Prevention of CNV formation may be important in maintaining visual function. Current preventive advice includes a suggestion for not to smoke, and possibly information regarding various supplementations; however, further preventive strategies are needed. Our data suggest that the use of pitavastatin could be helpful in

preventing CNV development in AMD patients. Furthermore, a prospective randomized controlled trial is needed to definitely address the question of statins and AMD.

References

Ambati, J., Anand, A., Fernandez, S., Sakurai, E., Lynn, B.C., Kuziel, W.A., Rollins, B.J., Ambati, B.K., 2003. An animal model of age-related macular degeneration in senescent Ccl-2- or Ccr-2-deficient mice. Nat. Med. 9, 1390–1397.

Bellosta, S., Ferri, N., Bernini, F., Paoletti, R., Corsini, A., 2000. Non-lipid-related effects of statins. Ann. Med. 32, 164–176.

Delcourt, C., Michel, F., Colvez, A., Lacroux, A., Delage, M., Vernet, M.H., 2001. Associations of cardiovascular disease and its risk factors with age-related macular degeneration: the POLA study. Ophthalmic. Epidemiol. 8, 237–249.

Edelman, J.L., Castro, M.R., 2000. Quantitative image analysis of laser-induced choroidal neovascularization in rat. Exp. Eye Res. 71, 523–533.

Fine, S.L., Berger, J.W., Maguire, M.G., Ho, A.C., 2000. Age-related macular degeneration. N. Engl. J. Med. 342, 483–492.

Frick, M., Dulak, J., Cisowski, J., Jozkowicz, A., Zwick, R., Alber, H., Dichtl, W., Schwarzacher, S.P., Pachinger, O., Weidinger, F., 2003. Statins differentially regulate vascular endothelial growth factor synthesis in endothelial and vascular smooth muscle cells. Atherosclerosis 170, 229–236.

Grossniklaus, H.E., Ling, J.X., Wallace, T.M., Dithmar, S., Lawson, D.H., Cohen, C., Elner, V.M., Elner, S.G., Sternberg Jr., P., 2002. Macrophage and retinal pigment epithelium expression of angiogenic cytokines in choroidal neovascularization. Mol. Vis. 8, 119–126.

Hall, N.F., Gale, C.R., Syddall, H., Phillips, D.I., Martyn, C.N., 2001. Risk of macular degeneration in users of statins: cross sectional study. BMJ 323, 375–376.

Hess, D.C., Fagan, S.C., 2001. Pharmacology and clinical experience with simvastatin. Expert Opin. Pharmacother. 2, 153–163.

Honjo, M., Tanihara, H., Nishijima, K., Kiryu, J., Honda, Y., Yue, B.Y., Sawamura, T., 2002. Statin inhibits leukocyte–endothelial interaction and prevents neuronal death induced by ischemia-reperfusion injury in the rat retina. Arch. Ophthalmol. 120, 1707–1713.

Jialal, I., Stein, D., Balis, D., Grundy, S.M., Adams-Huet, B., Devaraj, S., 2001. Effect of hydroxymethyl glutaryl coenzyme a reductase inhibitor therapy on high sensitive C-reactive protein levels. Circulation 103, 1933–1935.

Klaver, C.C., Assink, J.J., van Leeuwen, R., Wolfs, R.C., Vingerling, J.R., Stijnen, T., Hofman, A., de Jong, P.T., 2001. Incidence and progression rates of age-related maculopathy: the Rotterdam Study. Invest. Ophthalmol. Vis. Sci. 42, 2237–2241.

Klein, R., Klein, B.E., Tomany, S.C., Danforth, L.G., Cruickshanks, K.J., 2003. Relation of statin use to the 5-year incidence and progression of age-related maculopathy. Arch. Ophthalmol. 121, 1151–1155.

Kvanta, A., Algvere, P.V., Berglin, L., Seregard, S., 1996. Subfoveal fibrovascular membranes in age-related macular degeneration express vascular endothelial growth factor. Invest. Ophthalmol. Vis. Sci. 37, 1929–1934.

Kwak, B., Mulhaupt, F., Veillard, N., Pelli, G., Mach, F., 2001. The HMG-CoA reductase inhibitor simvastatin inhibits IFN-gamma induced MHC class II expression in human vascular endothelial cells. Swiss. Med. Wkly. 131, 41–46.

Lopez, P.F., Sippy, B.D., Lambert, H.M., Thach, A.B., Hinton, D.R., 1996. Transdifferentiated retinal pigment epithelial cells are immunoreactive for vascular endothelial growth factor in surgically excised age-related macular degeneration-related choroidal neovascular membranes. Invest. Ophthalmol. Vis. Sci. 37, 855–868.

Mahley, R.W., Huang, Y., Rall Jr., S.C., 1999. Pathogenesis of type III hyperlipoproteinemia (dysbetalipoproteinemia). Questions, quandaries, and paradoxes. J. Lipid Res. 40, 1933–1949.

McCarty, C.A., Mukesh, B.N., Fu, C.L., Mitchell, P., Wang, J.J., Taylor, H.R., 2001. Risk factors for age-related maculopathy: the Visual Impairment Project. Arch. Ophthalmol. 119, 1455–1462.

McGwin Jr., G., Modjarrad, K., Hall, T.A., Xie, A., Owsley, C., 2006. 3-hydroxy-3-methylglutaryl coenzyme a reductase inhibitors and the presence of age-related macular degeneration in the Cardiovascular Health Study. Arch. Ophthalmol. 124, 33–37.

McGwin Jr., G., Owsley, C., Curcio, C.A., Crain, R.J., 2003. The association between statin use and age related maculopathy. Br. J. Ophthalmol. 87, 1121–1125.

Mesri, M., Liversidge, J., Forrester, J.V., 1994. ICAM-1/LFA-1 interactions in T-lymphocyte activation and adhesion to cells of the blood–retina barrier in the rat. Immunology 83, 52–57.

Mitchell, P., Smith, W., Attebo, K., Wang, J.J., 1995. Prevalence of age-related maculopathy in Australia. The Blue Mountains Eye Study. Ophthalmology 102, 1450–1460.

Mitchell, P., Wang, J.J., Smith, W., Leeder, S.R., 2002. Smoking and the 5-year incidence of age-related maculopathy: the Blue Mountains Eye Study. Arch. Ophthalmol. 120, 1357–1363.

Plenge, J.K., Hernandez, T.L., Weil, K.M., Poirier, P., Grunwald, G.K., Marcovina, S.M., Eckel, R.H., 2002. Simvastatin lowers C-reactive protein within 14 days: an effect independent of low-density lipoprotein cholesterol reduction. Circulation 106, 1447–1452.

Pruefer, D., Scalia, R., Lefer, A.M., 1999. Simvastatin inhibits leukocyte–endothelial cell interactions and protects against inflammatory processes in normocholesterolemic rats. Arterioscler. Thromb. Vasc. Biol. 19, 2894–2900.

Romano, M., Diomede, L., Sironi, M., Massimiliano, L., Sottocorno, M., Polentarutti, N., Guglielmotti, A., Albani, D., Bruno, A., Fruscella, P., Salmona, M., Vecchi, A., Pinza, M., Mantovani, A., 2000. Inhibition of monocyte chemotactic protein-1 synthesis by statins. Lab. Invest. 80, 1095–1100.

Sakurai, E., Taguchi, H., Anand, A., Ambati, B.K., Gragoudas, E.S., Miller, J.W., Adamis, A.P., Ambati, J., 2003. Targeted disruption of the CD18 or ICAM-1 gene inhibits choroidal neovascularization. Invest. Ophthalmol. Vis. Sci. 44, 2743–2749.

Semkova, I., Peters, S., Welsandt, G., Janicki, H., Jordan, J., Schraermeyer, U., 2003. Investigation of laser-induced choroidal neovascularization in the rat. Invest. Ophthalmol. Vis. Sci. 44, 5349–5354.

Shen, W.Y., Yu, M.J., Barry, C.J., Constable, I.J., Rakoczy, P.E., 1998. Expression of cell adhesion molecules and vascular endothelial growth factor in experimental choroidal neovascularisation in the rat. Br. J. Ophthalmol. 82, 1063–1071.

Takehana, Y., Kurokawa, T., Kitamura, T., Tsukahara, Y., Akahane, S., Kitazawa, M., Yoshimura, N., 1999. Suppression of laser-induced choroidal neovascularization by oral tranilast in the rat. Invest. Ophthalmol. Vis. Sci. 40, 459–466.

Takemoto, M., Liao, J.K., 2001. Pleiotropic effects of 3-hydroxy-3-methylglutaryl coenzyme a reductase inhibitors. Arterioscler. Thromb. Vasc. Biol. 21, 1712–1719.

Tanemura, M., Miyamoto, N., Mandai, M., Kamizuru, H., Ooto, S., Yasukawa, T., Takahashi, M., Honda, Y., 2004. The role of estrogen and estrogen receptorbeta in choroidal neovascularization. Mol. Vis. 10, 923–932.

Urbich, C., Dernbach, E., Zeiher, A.M., Dimmeler, S., 2002. Double-edged role of statins in angiogenesis signaling. Circ. Res. 90, 737–744.

Vaughan, C.J., Gotto Jr., A.M., Basson, C.T., 2000. The evolving role of statins in the management of atherosclerosis. J. Am. Coll. Cardiol. 35, 1–10.

Wassmann, S., Faul, A., Hennen, B., Scheller, B., Bohm, M., Nickenig, G., 2003. Rapid effect of 3-hydroxy-3-methylglutaryl coenzyme a reductase inhibition on coronary endothelial function. Circ. Res. 93, e98–e103.

Weis, M., Heeschen, C., Glassford, A.J., Cooke, J.P., 2002. Statins have biphasic effects on angiogenesis. Circulation 105, 739–745.

Wilson, H.L., Schwartz, D.M., Bhatt, H.R., McCulloch, C.E., Duncan, J.L., 2004. Statin and aspirin therapy are associated with decreased rates of choroidal neovascularization among patients with age-related macular degeneration. Am. J. Ophthalmol. 137, 615–624.

Yi, X., Ogata, N., Komada, M., Yamamoto, C., Takahashi, K., Omori, K., Uyama, M., 1997. Vascular endothelial growth factor expression in choroidal neovascularization in rats. Graefes Arch. Clin. Exp. Ophthalmol. 235, 313–319.

Zambarakji, H.J., Nakazawa, T., Connolly, E., Lane, A.M., Mallemadugula, S., Kaplan, M., Michaud, N., Hafezi-Moghadam, A., Gragoudas, E.S., Miller, J.W., 2006. Dose-dependent effect of pitavastatin on VEGF and angiogenesis in a mouse model of choroidal neovascularization. Invest. Ophthalmol. Vis. Sci. 47, 2623–2631.

Zarbin, M.A., 2004. Current concepts in the pathogenesis of age-related macular degeneration. Arch. Ophthalmol. 122, 598–614.

Graefes Arch Clin Exp Ophthalmol (2008) 246:51–59
DOI 10.1007/s00417-007-0666-6

BASIC SCIENCE

Y-27632, a Rho-associated protein kinase inhibitor, attenuates neuronal cell death after transient retinal ischemia

Akira Hirata · Masaru Inatani · Yasuya Inomata · Naoko Yonemura · Takahiro Kawaji · Megumi Honjo · Hidenobu Tanihara

Received: 18 January 2007 / Revised: 19 July 2007 / Accepted: 30 July 2007 / Published online: 31 August 2007

Abstract
Purpose Transient retinal ischemia induces the death of retinal neuronal cells. Postischemic damage is associated with the infiltration of leukocytes into the neural tissue through vascular endothelia. The current study aimed to investigate whether this damage was attenuated by the inhibition of Rho/ROCK (Rho kinases) signaling, recently shown to play a critical role in the transendothelial migration of leukocytes.
Methods Y-27632, a selective inhibitor of ROCK, was injected intravitreally into rat eyes with transient retinal ischemia. Cell loss of the ganglion cell layer (GCL) and thinning of the inner plexiform layer (IPL) with and without the administration of Y-27632 were evaluated by histological anaysis, TUNEL assay and retrograde labeling of retinal ganglion cells (RGCs). To examine the attenuation of leukocyte infiltration in postischemic retinas with the administration of Y-27632, silver nitrate staining and immunohistochemistry using an anti-LCA antibody were performed.
Results Cell loss of the GCL and thinning of the IPL were significantly attenuated when 100 nmol Y-27632 was administered within three hours of the induction of ischemia. TUNEL assay and retrograde labeling of RGCs showed a decreased number of apoptotic cells and an increased number of RGCs in Y-27632-injected retinas. Moreover, silver nitrate staining and immunohistochemical analysis using an anti-LCA antibody showed that Y-27632 injection dramatically inhibited leukocyte infiltration and endothelial disarrangement.
Conclusions Our data suggest that inhibition of Rho/ROCK signaling offers neuroprotective therapy against postischemic neural damage, by regulating leukocyte infiltration in the neural tissue.

Keywords Rho · Rho kinases · Ocular hypertension · Extravasation · Cytoskeleton · Retinal ischemia

A. Hirata · M. Inatani (✉) · Y. Inomata · N. Yonemura · T. Kawaji · H. Tanihara
Department of Ophthalmology and Visual Science,
Kumamoto University Graduate School of Medical Sciences,
1-1-1 Honjo,
Kumamoto 860-8556, Japan
e-mail: inatani@fc.kuh.kumamoto-u.ac.jp

M. Honjo
Department of Ophthalmology, Kitano Hospital,
Osaka, Japan

Introduction

Retinal ischemia leads to a loss of neuronal cells in the inner retinal layers such as retinal ganglion cells (RGCs) and amacrine cells [8, 49]. Human pathological conditions associated with inner retinal neuronal cell death, including central retinal artery occlusion [13, 53, 61] and glaucoma [23, 47], have been widely studied using animal models of retinal ischemia. Such models reproducibly induce inner retinal neuronal cell apoptosis.

Neuronal cell apoptosis induced by transient retinal ischemia progresses through the reperfusion phase rather than the ischemic phase. Injury during reperfusion is caused by the infiltration of leukocytes into the neural tissue through vascular endothelia [53, 54]. During the transendothelial migration of leukocytes known as extravasation, endothelial permeability and leukocyte adhesion to endothelial cells are affected by chemokines, their receptors, adhesion molecules, and cytoskeletal components [31, 38, 51, 59]. Recently, evidence has accumulated suggesting

that leukocyte extravasation is also associated with the pathological mechanisms of retinal diseases accompanied by persistent visual disturbance, such as age-related macular degeneration [2, 48, 60] and macular edema [42, 55]. These studies show that animal models of ischemic reperfusion are powerful tools for investigating the pathological processes of retinal neuronal cell death and leukocyte extravasation.

The small GTP-binding protein, Rho, contributes to leukocyte extravasation by regulating the leukocyte cytoskeleton and tight junction of endothelial cells [39, 57]. Rho promotes myosin light chain phosphorylation by activating downstream effecters, Rho kinases (ROCKs), resulting in actomyosin-based contraction and the formation of stress fibers [1, 44]. We therefore hypothesized that the Rho/ROCK signaling pathway would play a critical role in leukocyte extravasation after transient retinal ischemia. We predicted that inactivation of Rho/ROCK signaling would contribute to the neuroprotectivity of neuronal cells in the inner retina against the reperfusion injury. Indeed, a previous study showed that Y-27632, an inhibitor of ROCKs, attenuated leukocyte recruitment following cardiac ischemic-reperfusion damage, resulting in decreased cell loss in cardiac muscle [4]. We anticipated that the inhibition of Rho/ROCK signaling could lead to a therapeutic approach for retinal diseases. To this end, we evaluated the capacity of Y-27632 to inhibit leukocyte extravasation after transient retinal ischemia and attenuate postischemic neuronal cell death.

Materials and methods

Animals

Male Sprague-Dawley rats (8–12 weeks old, 180–200 g; Kyudo, Kumamoto, Japan) were used in this study. All experiments were performed in accordance with the Statement on the Use of Animals of the Association for Research in Vision and Ophthalmology. Transient ocular hypertension was induced in the right eye of each rat, according to the method of Rosenbaum et al. [49], with slight modifications. Rats were anesthetized with a 1:1 mixture of xylazine hydrochloride (4 mg/kg; Bayer Healthcare, Tokyo, Japan) and ketamine hydrochloride (10 mg/kg; Sankyo, Tokyo, Japan). Dilation of the pupil was achieved with 0.5% tropicamide and 2.5% phenylephrine hydrochloride (Santen, Osaka, Japan). The anterior chamber of the right eye was cannulated with a 30-gauge needle and the intraocular pressure (IOP) was raised to 130 mm Hg by infusing balanced salt solution through a line attached to the needle. Completed non-perfusion was confirmed via an operating microscope (Carl Zeiss Japan, Tokyo, Japan). After 60 min of ocular hypertension, the needle was withdrawn and the IOP was normalized. The operating microscope was also used to verify reperfusion of the vessels.

Chemicals and drug administration

The dosage effects of Y-27632 (Calbiochem-Novabiochem, San Diego, CA, USA) were evaluated by injecting 1, 10, or 100 nmol Y-27632 into the vitreous, using Hamilton syringe with a 30-gauge sharpened needle (Ito, Shizuoka, Japan) aided by microscopy, 5 min before the induction of ocular hypertension. The temporal effects of Y-27632 were analyzed by injecting 100 nmol Y-27632 at 5 min, 3 h, 6 h, 12 h, 24 h, or 48 h before the induced ocular hypertension. Each dosage of Y-27632 was diluted with phosphate buffered saline (PBS) to the same final volume (1 μl) for the intravitreal injection.

Histological analysis

Histological evaluation was performed as described previously [41]. Briefly, seven days after the induction of ocular hypertension, the rats were killed by an intraperitoneal overdose injection of pentobarbital (Dainippon Seiyaku, Osaka, Japan). The eyes were enucleated and immersed in a fixative containing 2.5% glutaraldehyde and 2% paraformaldehyde (PFA) in 0.1 M phosphate buffer (pH 7.4) for 24 h at 4°C, followed by dehydration and embedding in paraffin. Transverse, 4-μm thick sections were made through the optic disc, stained with hematoxylin and eosin, and subjected to histological analysis. The degree of hypertension-induced neuronal damage in the retina was quantified by means of cell counts in the ganglion cell layer (GCL) and by measuring the thickness of the inner plexiform layer (IPL), 1.5 mm from the optic disc. Three sections for each eye were randomly selected. The cell count in GCL and the thickness of IPL were averaged in the three sections. Eight eyes were performed in each experimental condition.

Terminal deoxyribonucleotidyl transferase (TdT)-mediated fluroscein-16-dUTP nick end-labeling (TUNEL) assay

It has previously been shown in a rat model of retinal ischemia-reperfusion injury by transient elevated IOP, that TUNEL-positive cells are clearly observed in the GCL and INL 18 hours after ischemia [36]. Therefore, to evaluate the effect of Y-27632 on the attenuation of apoptosis, eyes were enucleated 18 hours after ischemia induction, and fixed in 4% PFA in PBS (pH 7.4). The TUNEL assay was performed with apoptosis detection system fluorescein (Promega, Madison, WI). The specimens were then dehydrated and embedded in paraffin and 5-μm sections

were cut. TUNEL-positive cells were counted in the GCL, and the inner nuclear layer (INL) at 1.0 to 1.5 mm from the optic disc was measured. Four eyes were evaluated for each condition.

Retrograde labeling of retinal ganglion cells

Four days after ischemia induction, retrograde labeling of retinal ganglion cells (RGCs) was performed in a manner similar to that described previously [50]. The cell count of living RGCs was performed as previously described [28, 32, 33]. Briefly, after anesthesia, rat heads were fixed in a stereotaxic apparatus. Fluoro-Gold (Fluorochrome, Englewood, CO, USA) was microinjected bilaterally into the superior colliculus. Three days after the injection, the animals were killed by an intraperitoneally injected overdose of pentobarbital. Eyes were enucleated and fixed in 4% PFA for 1 h. Retinas were divided into six segments by means of radial cuts, removed from the sclera and mounted on slides. Regions used for counting the number of Fluoro-Gold-labeled RGCs were selected from two adjacent fields in the central area (1 mm from the optic disc) from each of the six radial cuts. Thus, for each eye, 12 fields were evaluated to obtain the labeled RGC counts. Four eyes were evaluated for each condition.

Silver nitrate staining of endothelial-leukocyte interaction

Nine eyes (three eyes in each condition) were used for light microscopic studies of silver-stained endothelial cells. Six hours after ischemia induction, rats were perfused through the aorta with fixative (1% PFA and 0.5% glutaraldehyde in 0.075 M cacodylate buffer, pH 7.4) for 5 min at a pressure of 120–140 mmHg. Thereafter, the vasculature was stained with silver by perfusing five solutions in rapid succession: first, 0.9% NaCl for 2 min; second, 5% glucose for 10 s; third, 0.2% $AgNO_3$ for 7 s; fourth, 5% glucose for 10 s; and fifth, fixative for 1 min. After perfusion, the eyes were removed, cut at the equator to make eyecups, and the silver was developed by exposure to light for 15 min. After silver staining, the retinas of the eyecups were cut radially, then dehydrated in ethanol, cleared in toluene, and mounted retinal surface up.

Immunohistochemistry of infiltrating leukocytes

Twelve eyes (four eyes in each condition) were used for light microscopic studies of extravasated leukocytes. Twenty-four hours after ischemia induction, eyes were enucleated and fixed. Cryosections were blocked with 3% H_2O_2 in methanol. Sections were blocked with 10% goat serum in PBS before incubation for 1 hour with the primary antibody, a mouse anti-rat monoclonal antibody for the leukocyte common antigen (LCA)/CD45 (Serotec, Oxford, UK). Sections were then incubated for one hour with the secondary antibody, a horseradish peroxidase-conjugated goat anti-mouse IgG antibody (DAKO Japan, Kyoto, Japan). 3,3′-diaminobenzidine, tetrahydrochloride (DAB; DAKO Japan) was used as a chromogen. Cells that stained positive for LCA were counted.

Statistical analysis

Y-27632 dose effect and time course effect values were presented as means ± SE. TUNEL assay, retrograde RGC labeling and infiltrating leukocyte immunohistochemistry values were presented as means ± SD. Data were analyzed by one-way analysis of variance (ANOVA) using the post-hoc test with Fisher's protected least significant difference procedure. Differences were considered statistically significant when p-values were less than 0.05.

Results

Morphometric analysis of the neuroprotective effect of Y-27632

To investigate the protective effects of Y-27632 against retinal ischemia induced by 60 min of ocular hypertension (130 mm Hg), we performed a quantitative morphometric analysis (Fig. 1). The transient retinal ischemia was shown to have caused severe destruction of the inner retinal elements, which decreased the retinal thickness and damaged the retinal cells (Fig. 1a).

In PBS-treated eyes with ischemia, the mean cell density in the GCL was 29.8±1.8 cells/mm, which was significantly lower than the mean cell density of control retinas without ischemia (53.8±1.0 cells/mm; $p<0.0001$; Fig. 1b). Moreover, the mean IPL thickness in PBS-treated rats with ischemia (27.4±5.5 μm) was significantly reduced compared with retinas without ischemia (43.3±1.3 μm; $p<0.0001$; Fig. 1c). Compared with PBS-treated eyes with ischemia, the injection of 100 nmol Y-27632 before the induction of transient retinal ischemia resulted in significant protection against ischemic damage, as shown by the rescue of GCL mean cell number (37.7±1.1 cells/mm, $p=0.0021$; Fig. 1b) and mean IPL thickness (32.8±2.0 μm, $p=0.022$; Fig. 1c). No significant effect on GCL cell number or IPL thickness was induced by injections of either 1 nmol or 10 nmol Y-27632.

To evaluate the timing of Y-27632 administration, 100 nmol Y-27632 was given at 5 min, 3 h, 6 h, 12 h, 24 h, or 48 h before the induction of hypertension. Significant protection from ischemic damage was provided by treatment with Y-27632 5 min and 3 h prior to the induction of ischemia, compared

with control PBS-treated eyes (GCL cell count 37.7±1.1, p=0.002 and 36.0±1.5, p=0.033 respectively; Fig. 2a). Similarly, IPL thickness was significantly higher in eyes treated with Y-27632 5 min and 3 h prior to ischemia induction, compared with control PBS-treated eyes (p=0.031 and p=0.003 respectively; Fig. 2b).

Neuroprotective effects of Y-27632 evaluated by the TUNEL assay

Few TUNEL-positive cells were observed in retinas without ischemia (Fig. 3a) but, 18 hours after ischemia induction, numerous TUNEL-positive cells (mean 36.6±12.7 cells/mm) were found in the GCL and the inner nuclear layer (INL) (Fig. 3b). After treatment with 100 nmol Y-27632, the number of TUNEL-positive cells in the GCL and INL was significantly decreased (mean 20.6±1.4 cells/mm, p=0.015; Fig. 3c,d).

Analysis of the protective effects of Y-27632 by retrograde labeling of RGCs

To determine whether Y-27632 can protect from ischemia, retrograde labeling of RGCs was performed using Fluoro-Gold. The mean RGC density in eyes without ischemia was

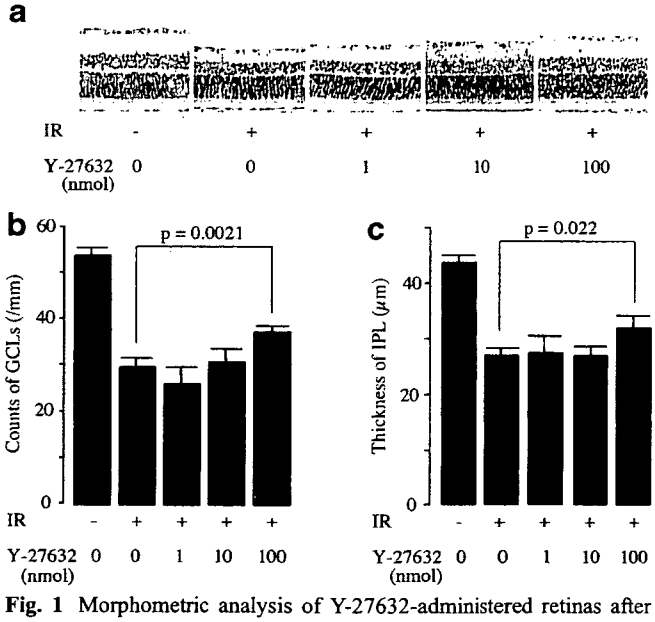

Fig. 1 Morphometric analysis of Y-27632-administered retinas after induction of transient ischemia. **a** Transverse sections stained with hematoxylin and eosin. Intravitreal injection of various concentrations of Y-27632 was performed 5 min before the induction of ocular hypertension. **b** The mean GCL cell density (/mm) at each Y-27632 concentration. **c** The mean IPL thickness (μm) at each Y-27632 concentration. Eight eyes were performed in each experimental condition. *IR*: ischemic retinal damage; +: with ischemia; −: without ischemia; *error bar*: ± SE

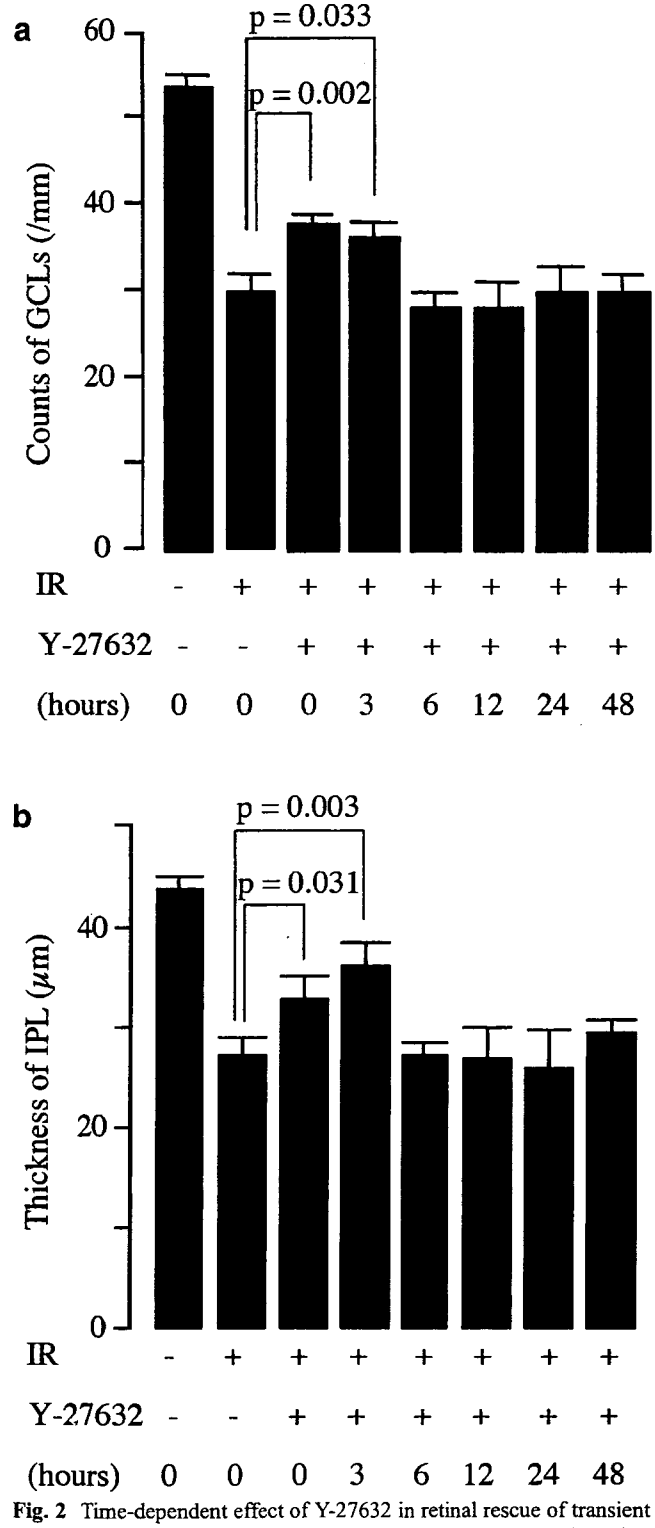

Fig. 2 Time-dependent effect of Y-27632 in retinal rescue of transient retinal ischemia. A time course of Y-27632 was evaluated by injecting 100 nmol Y-27632 at 5 min, 3 h, 6 h, 12 h, 24 h, or 48 h before induced ocular hypertension. A significant rescue of GCL cell number (**a**) and IPL thickness (**b**) was observed following administration at 5 min and 3 h prior to retinal ischemia. Eight eyes were performed in each experimental condition. *IR*: ischemic retinal damage; +: with ischemia; −: without ischemia; *error bar*: ± SE

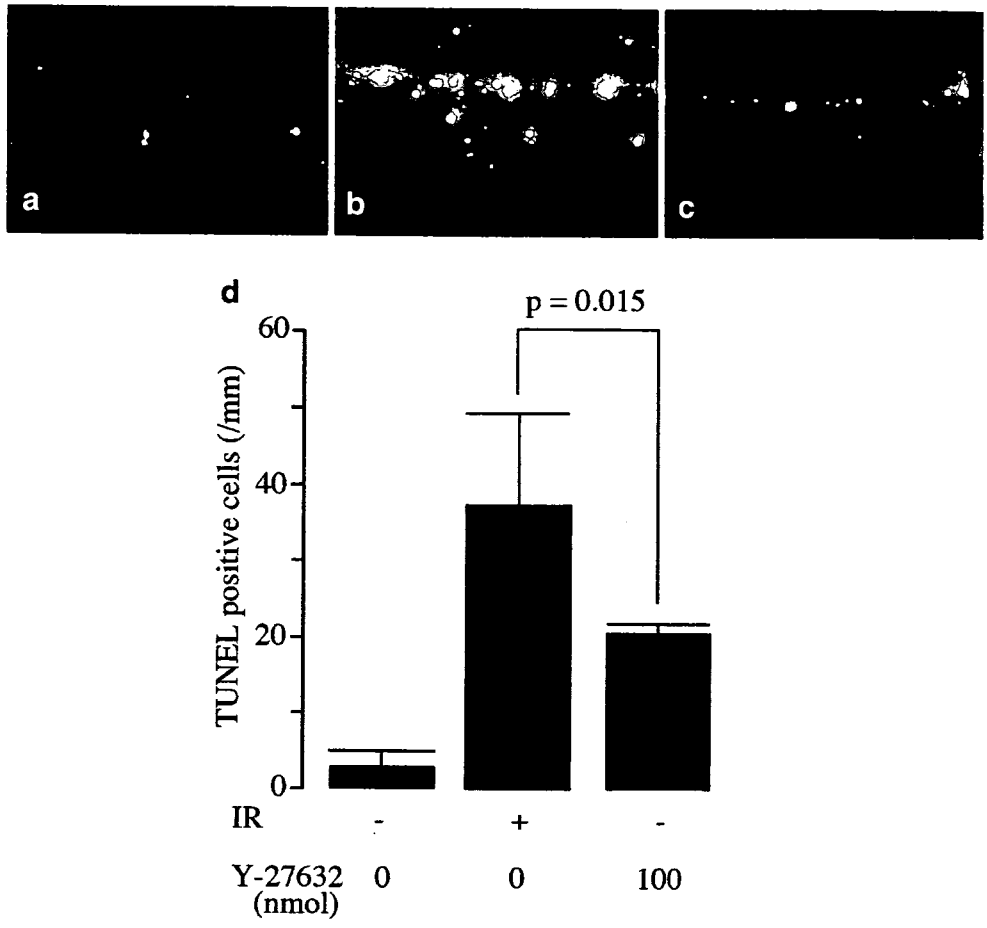

Fig. 3 Decreased number of TUNEL-positive cells in Y-27632-administered retina. Few TUNEL-positive cells were detected in retinal sections that had not undergone ischemia (**a**). Transient retinal ischemia induced TUNEL-positive cells in the GCL and INL (**b**), while administration of 100 nmol Y-27632 decreased the number of positive cells (**c**). TUNEL-positive cells were counted following each treatment (n=4) and Y-27632 shown to significantly decrease their number (**d**). *IR*: ischemic retinal damage; +: with ischemia; −: without ischemia; *error bar*: ± SE

1169.8±92.1 cells/mm^2 (Fig. 4a,d). Four days after ischemia induction, the mean density of labeled RGCs had fallen to 610.2±146.4 cells/mm^2 (Fig. 4b,d). Intravitreal injection of 100 nmol Y-27632 significantly protected RGCs against retinal ischemia, resulting in a mean RGC density of 784.7± 65.9 cells/mm^2 (p=0.015; Fig. 4c,d).

Silver nitrate staining and immunohistochemistry for infiltrating leukocytes

Endothelial cell borders were clearly stained with silver nitrate in retinal vessels without ischemia (Fig. 5a). After ischemia induction, numerous silver dots and rings, representing endothelial gaps and adherent leukocytes, respectively, were observed as previously reported [36] (Fig. 5b). Treatment with 100 nmol Y-27632 decreased the number of silver dots and rings (Fig. 5c). Few LCA-positive cells were observed in retinas without ischemia (Fig. 5d), but they increased abundantly 24 hours after ischemia induction (197.7±44.7 cells/mm; Fig. 5e,g). Treatment with 100 nmol Y-27632 decreased the number of LCA-positive cells (71.1±48.3 cells/mm; Fig. 5f,g) and the decrease was shown to be significant (p=0.007; Fig. 5g).

Discussion

The present study has demonstrated that intravitreal injection of the ROCK inhibitor Y-27632 attenuates the loss of retinal cells in the inner retinal layers after transient retinal ischemia, and that Y-27632 suppresses leukocyte recruitment and the disturbance of vascular endothelial cell alignment in the postischemic retina. Our data suggest that Y-27632 may inhibit retinal damage through regulating leukocyte infiltration in the retinal tissue. As reported previously, transient retinal ischemia induces the loss of retinal neuronal cells, especially in the inner retinal layers such as GCL and INL [46, 52]. Our ocular hypertension model, in which ischemic reperfusion in the retinal vessels has been confirmed microscopically, also drastically decreases the cell number of the GCL and the IPL thickness at 7 days after transient retinal ischemia, as described in previous reports [15, 45, 49], reflecting the destruction of the inner retinal elements.

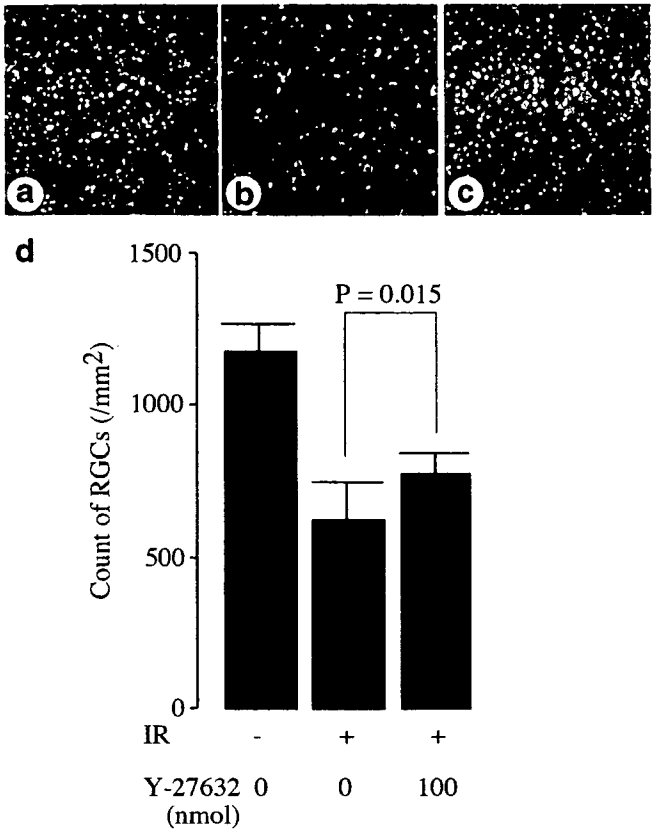

Fig. 4 Rescued RGCs in Y-27632-administered retina. Retrograde labeling of RGCs in the intact retina (**a**) by fluorescent crystal. The number of labeled RGCs decreased after transient retinal ischemia (**b**). In contrast, the number was restored by Y-27632 administration 5 min before the induction of retinal ischemia (**c**). The cell density (/mm^2) was evaluated in each condition (n=4) (**d**). +: with ischemia; −: without ischemia

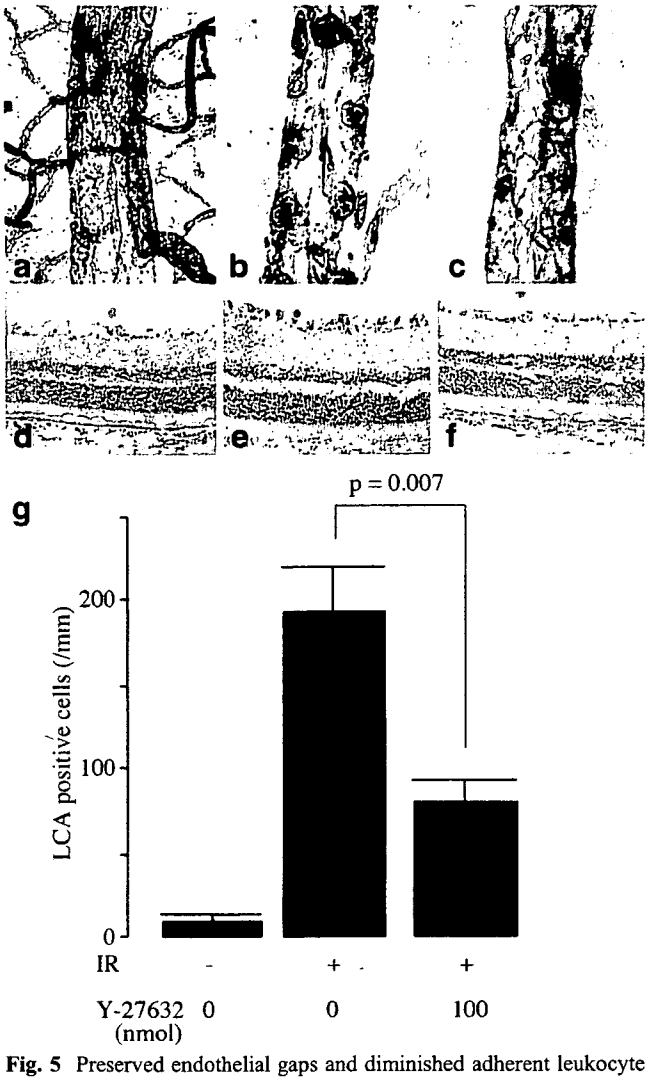

Fig. 5 Preserved endothelial gaps and diminished adherent leukocyte numbers in Y-27632-administered retinal vessels. Silver nitrate-stained endothelial cell borders in normal retinal vessels (**a**). Retinal vessels after transient ischemia demonstrated numerous silver dots and rings (**b**), which represent endothelial gaps and adherent leukocytes, respectively. Administration of Y-27632 attenuated the number of endothelial gaps and adherent leukocytes in ischemic retinal vessels (**c**). Silver nitrate-staining was performed in four eyes in each condition. LCA-positive cells (leukocytes) were few in number in normal retinal sections (**d**), while numerous immuno-positive cells were observed in the GCL after induction of transient ischemia (**e**). Administration of Y-27632 decreased the number of LCA-positive cells in the transient ischemic retina (**f**). LCA-positive cells were counted following each treatment (n=4) and 100 nmol Y-27632 was shown to significantly decrease their numbers (**g**). +: with ischemia; −: without ischemia

Recent studies have revealed that apoptosis is involved in neuronal cell death after ischemia [8, 35, 37]. Indeed, in our animal model, a significant number of TUNEL-positive cells were observed in the GCL and INL at 18 h after reperfusion, indicating apoptosis of the inner retinal cells after transient ischemia. As described previously [16, 36], TUNEL-positive cells are detected in the inner retinal layers at an early period, between 4 h and 24 h after reperfusion. These results suggest that ocular hypertension induces postischemic neuronal cell apoptosis in the GCL and INL. In contrast, when Y-27632 is administered intraviteally, cell loss and the number of apoptotic cells in the inner retina was significantly reduced. Fluoro-Gold dye is one of the most effective labeling-tracers and has been shown to label RGCs in a pair of eyes with a variance of just 4.1% [12]. Our labeling did, however, confirm that Y-27632 reduces the loss of RGCs by 28.6% after the induction of transient ischemia. Together, our data clearly demonstrate the neuroprotective effect of Y-27632 on postischemic retinal neuronal cell death.

Regarding the mechanisms of retinal damage after ischemia, leukocyte adherence to the vascular endothelium and the subsequent infiltration into postischemic tissues are reported to contribute to neuronal cell death in the postischemic area [11, 30]. Infiltrated leukocytes release oxidants and proteases, exhibiting inflammatory reactions that further increase the damage to postischemic tissue [34]. Accumulating evidence suggests that the neutralization of leukocyte

activation or the suppressed expression of leukocyte adhesion molecules on the vascular endothelial surface reduce postischemic damage and inhibit leukocyte-endothelium interaction [22, 29, 56]. The signaling pathway of Rho GTPases and their downstream effecter, ROCK, is involved in the regulation of cell motility, adhesion, and cytokinesis through the reorganization of the actin cytoskeleton and, as such, plays a critical role in leukocyte-endothelium interaction [39, 59]. It has been reported that increased expression of Rho and activation of ROCK are observed in ischemic-reperfusion tissue [4]. Moreover, a recent in vivo study demonstrated that a ROCK inhibitor reduces the infiltration of inflammatory cells into lung tissue in leukocyte-activated animal models [24]. Similarly, our present data demonstrate that injection of Y-27632 decreases the number of LCA-positive cells, indicating a decrease of recruited leukocytes in the postischemic retinal tissue. Our silver staining data also support a decrease in the number of leukocytes recruited in Y-27632-injected eyes. Although our data don't exclude the possibility that Y-27632 is neuroprotective even in the ischemic phase before reperfusion, Y-27632-induced inhibition of leukocyte activation in retinal vessels after reperfusion may attenuate neuronal cell death in the inner retinal layers.

In addition to the effects of Rho GTPases on leukocyte activation by modification of their cytoskeleton, Rho GTPase signaling pathways regulate the integrity of intercellular junctions in vascular endothelial cells, leading to accelerated trans-endothelial migration of leukocytes [17, 18, 27, 58]. Interestingly, silver staining in the postischemic retina demonstrated that the number of endothelial gaps is reduced following injection of Y-27632. This effect on the disarrangement of endothelial cells may be associated with the inhibition of Rho/ROCK signaling in endothelial cells.

The neuroprotective effect of Y-27632 is significantly observed only when the drug is administered during the early period before ischemia. We previously showed that leukocyte-endothelial cell interaction is initiated within 4 hours of reperfusion [43]. It has also been reported that Rho expression is increased 4 hours after reperfusion in an ischemic-reperfusion heart [4], indicating that Rho/ROCK signaling is activated immediately after reperfusion. It was recently reported that hydrogen peroxide, one of the neurotoxic factors secreted by leukocytes, is produced within 30 minutes of retinal reperfusion [25]. This suggests that the degenerative process involving leukocyte infiltration starts immediately after transient ischemia. Therefore, we examined whether leukocyte infiltration was attenuated by Y-27632 in the early phase after reperfusion. These previous reports are consistent with our present data and with the hypothesis that a neuroprotective effect of Y-27632 is exhibited by its attenuation of leukocyte infiltration in postischemic retinal tissues.

However, we cannot exclude the possibility that neuroprotection is exhibited through a direct inhibition of Rho/ROCK signaling within retinal neuronal cells. Interestingly, many in vitro and in vivo studies have demonstrated that Y-27632 promotes the re-growth or sprouting of injured neural fibers [7, 9, 14, 21, 40]. However, no reports have described the direct neuroprotective effects of Y-27632 in vitro. In addition, a previous study observed no direct protective effect of Y-27632 in isolated postischemic rat hearts, despite the clear demonstration of a protective effect of Y-27632 on ischemic heart muscle cells in vivo [4]. Bertrand et al. [6] reported that the intravitreal injection of the Rho antagonist C3-07 promoted the survival of RGCs as well as regeneration in the axotomized rat optic nerve. They speculated that C3-07 might have activated Müller cells that in turn influenced RGC survival. These data show that direct inhibition of Rho/ROCK signaling within neuronal cells may be associated with axon regeneration, rather than a neuroprotective effect. ROCK inhibition in leukocytes and endothelial cells may play a critical role in the neuroprotective effect of Y-27632.

We have previously reported that topical administration of Y-27632 causes IOP reduction in rabbit eyes, eliciting increased aqueous outflow via trabecular meshwork and Schlemm's canal pathway [26]. Therefore, topical administration of Y-27632 is potential for the treatment of glaucoma, in which high IOP is a major risk factor for optical damage. It has been suggested that IOP elevation results in insufficient vascular blood flow around the optic nerve head. Many studies have demonstrated ischemia at the optic nerve as a component of glaucomatous optic neuropathy [3, 5, 10, 19, 20]. Our results suggest that Rho/ROCK signaling may be a promising target for the treatment of glaucoma optic neuropathy, as its inhibition is associated not only with IOP lowering, but also with a neuroprotective effect against ischemia-induced retinal cell death.

Acknowledgements This study was supported in part by Grants-in-Aid for Scientific Research from the Ministry of Education, Science, Sports and Culture, Japan, and from the Ministry of Health and Welfare, Japan.

References

1. Amano M, Fukata Y, Kaibuchi K (2000) Regulation and functions of Rho-associated kinase. Exp Cell Res 261:44–51
2. Anderson DH, Mullins RF, Hageman GS, Johnson LV (2002) A role for local inflammation in the formation of drusen in the aging eye. Am J Ophthalmol 134:411–431
3. Anderson DR (1999) Introductory comments on blood flow autoregulation in the optic nerve head and vascular risk factors in glaucoma. Surv Ophthalmol 43:S5–S9

4. Bao W, Hu E, Tao L, Boyce R, Mirabile R, Thudium DT, Ma XL, Willette RN, Yue TL (2004) Inhibition of Rho-kinase protects the heart against ischemia/reperfusion injury. Cardiovasc Res 61:548–558
5. Bechetoille A (1996) Vascular risk factors in glaucoma. Curr Opin Ophthalmol 7:39–43
6. Bertrand J, Winton MJ, Rodriguez-Hernandez N, Campenot RB, McKerracher L (2005) Application of Rho antagonist to neuronal cell bodies promotes neurite growth in compartmented cultures and regeneration of retinal ganglion cell axons in the optic nerve of adult rats. J Neurosci 25:1113–1121
7. Borisoff JF, Chan CC, Hiebert GW, Oschipok L, Robertson GS, Zamboni R, Steeves JD, Tetzlaff W (2003) Suppression of Rho-kinase activity promotes axonal growth on inhibitory CNS substrates. Mol Cell Neurosci 22:405–416
8. Buchi ER (1992) Cell death in the rat retina after a pressure-induced ischaemia-reperfusion insult: an electron microscopic study. I. Ganglion cell layer and inner nuclear layer. Exp Eye Res 55:605–613
9. Chan CC, Khodarahmi K, Liu J, Sutherland D, Oschipok LW, Steeves JD, Tetzlaff W (2005) Dose-dependent beneficial and detrimental effects of ROCK inhibitor Y27632 on axonal sprouting and functional recovery after rat spinal cord injury. Exp Neurol 196:352–364
10. Chung HS, Harris A, Evans DW, Kagemann L, Garzozi HJ, Martin B (1999) Vascular aspects in the pathophysiology of glaucomatous optic neuropathy. Surv Ophthalmol 43:S43–S50
11. Clark WM, Lutsep HL (2001) Potential of anticytokine therapies in central nervous system ischaemia. Expert Opin Biol Ther 1:227–237
12. Danias J, Shen F, Goldblum D, Chen B, Ramos-Esteban J, Podos SM, Mittag T (2002) Cytoarchitecture of the retinal ganglion cells in the rat. Invest Ophthalmol Vis Sci 43:587–594
13. Daugeliene L, Niwa M, Hara A, Matsuno H, Yamamoto T, Kitazawa Y, Uematsu T (2000) Transient ischemic injury in the rat retina caused by thrombotic occlusion-thrombolytic reperfusion. Invest Ophthalmol Vis Sci 41:2743–2747
14. Dergham P, Ellezam B, Essagian C, Avedissian H, Lubell WD, McKerracher L (2002) Rho signaling pathway targeted to promote spinal cord repair. J Neurosci 22:6570–6577
15. Dijk F, Kamphuis W (2004) Ischemia-induced alterations of AMPA-type glutamate receptor subunit. Expression patterns in the rat retina-an immunocytochemical study. Brain Res 997:207–221
16. Dijk F, Kamphuis W (2004) An immunocytochemical study on specific amacrine cell subpopulations in the rat retina after ischemia. Brain Res 1026:205–217
17. Essler M, Amano M, Kruse HJ, Kaibuchi K, Weber PC, Aepfelbacher M (1998) Thrombin inactivates myosin light chain phosphatase via Rho and its target Rho kinase in human endothelial cells. J Biol Chem 273:21867–21874
18. Essler M, Retzer M, Bauer M, Heemskerk JW, Aepfelbacher M, Siess W (1999) Mildly oxidized low density lipoprotein induces contraction of human endothelial cells through activation of Rho/Rho kinase and inhibition of myosin light chain phosphatase. J Biol Chem 274:30361–30364
19. Flammer J (1994) The vascular concept of glaucoma. Surv Ophthalmol 38:S3–S6
20. Flammer J, Orgul S, Costa VP, Orzalesi N, Krieglstein GK, Serra LM, Renard JP, Stefansson E (2002) The impact of ocular blood flow in glaucoma. Prog Retin Eye Res 21:359–393
21. Fournier AE, Takizawa BT, Strittmatter SM (2003) Rho kinase inhibition enhances axonal regeneration in the injured CNS. J Neurosci 23:1416–1423
22. Gidday JM, Gasche YG, Copin JC, Shah AR, Perez RS, Shapiro SD, Chan PH, Park TS (2005) Leukocyte-derived matrix metalloproteinase-9 mediates blood-brain barrier breakdown and is proinflammatory after transient focal cerebral ischemia. Am J Physiol Heart Circ Physiol 289:H558–H568
23. Hara H, Ichikawa M, Oku H, Shimazawa M, Araie M (2005) Bunazosin, a selective alpha1-adrenoceptor antagonist, as an anti-glaucoma drug: effects on ocular circulation and retinal neuronal damage. Cardiovasc Drug Rev 23:43–56
24. Hashimoto T, Yamashita M, Ohata H, Momose K (2003) Lysophosphatidic acid enhances in vivo infiltration and activation of guinea pig eosinophils and neutrophils via a Rho/Rho-associated protein kinase-mediated pathway. J Pharmacol Sci 91:8–14
25. Hirooka K, Miyamoto O, Jinming P, Du Y, Itano T, Baba T, Tokuda M, Shiraga F (2006) Neuroprotective effects of D-allose against retinal ischemia-reperfusion injury. Invest Ophthalmol Vis Sci 47:1653–1657
26. Honjo M, Tanihara H, Inatani M, Kido N, Sawamura T, Yue BY, Narumiya S, Honda Y (2001) Effects of rho-associated protein kinase inhibitor Y-27632 on intraocular pressure and outflow facility. Invest Ophthalmol Vis Sci 42:137–144
27. Hordijk PL, ten Klooster JP, van der Kammen RA, Michiels F, Oomen LC, Collard JG (1997) Inhibition of invasion of epithelial cells by Tiam1-Rac signaling. Science 278:1464–1466
28. Inomata Y, Hirata A, Yonemura N, Koga T, Kido N, Tanihara H (2003) Neuroprotective effects of interleukin-6 on NMDA-induced rat retinal damage. Biochem Biophys Res Commun 302:226–232
29. Ishikawa M, Cooper D, Russell J, Salter JW, Zhang JH, Nanda A, Granger DN (2003) Molecular determinants of the prothrombogenic and inflammatory phenotype assumed by the postischemic cerebral microcirculation. Stroke 34:1777–1782
30. Ishikawa M, Zhang JH, Nanda A, Granger DN (2004) Inflammatory responses to ischemia and reperfusion in the cerebral microcirculation. Front Biosci 9:1339–1347
31. Johnson-Leger C, Aurrand-Lions M, Imhof BA (2000) The parting of the endothelium: miracle, or simply a junctional affair? J Cell Sci 113:921–933
32. Kido N, Tanihara H, Honjo M, Inatani M, Tatsuno T, Nakayama C, Honda Y (2000) Neuroprotective effects of brain-derived neurotrophic factor in eyes with NMDA-induced neuronal death. Brain Res 884:59–67
33. Kido N, Inatani M, Honjo M, Yoneda S, Hara H, Miyawaki N, Honda Y, Tanihara H (2001) Dual effects of interleukin-1beta on N-methyl-D-aspartate-induced retinal neuronal death in rat eyes. Brain Res 910:153–162
34. Kontos CD, Wei EP, Williams JI, Kontos HA, Povlishock JT (1992) Cytochemical detection of superoxide in cerebral inflammation and ischemia in vivo. Am J Physiol 263:H1234–H1242
35. Kuroiwa S, Katai N, Shibuki H, Kurokawa T, Umihira J, Nikaido T, Kametani K, Yoshimura N (1998) Expression of cell cycle-related genes in dying cells in retinal ischemic injury. Invest Ophthalmol Vis Sci 39:610–661
36. Lam TT, Abler AS, Tso MO (1999) Apoptosis and caspases after ischemia-reperfusion injury in rat retina. Invest Ophthalmol Vis Sci 40:967–975
37. Levin LA, Louhab A (1996) Apoptosis of retinal ganlion cells in anterior ischemic optic neuropathy. Arch Ophthalmol 114:488–491
38. McDonald DM (1994) Endothelial gaps and permeability of venules in rat tracheas exposed to inflammatory stimuli. Am J Physiol 266:L61–L83
39. Millán J, Ridley AJ (2005) Free in PMC Rho GTPases and leucocyte-induced endothelial remodelling. Biochem J 385:329–337
40. Monnier PP, Sierra A, Schwab JM, Henke-Fahle S, Mueller BK (2003) The Rho/ROCK pathway mediates neurite growth-inhibitory activity associated with the chondroitin sulfate proteoglycans of the CNS glial scar. Mol Cell Neurosci 22:319–330